AD-A032 264 HUGHES RESEARCH LABS MALIBU CALIF F/G 20/5
OPTIMIZED THIN FILM LIGHT SOURCES.(U)
SEP 76 R G HUNSPERGER, A YARIV F33615-75-C-1024
UNCLASSIFIED AFAL-TR-76-81 NL

| OF |
AD
A032264

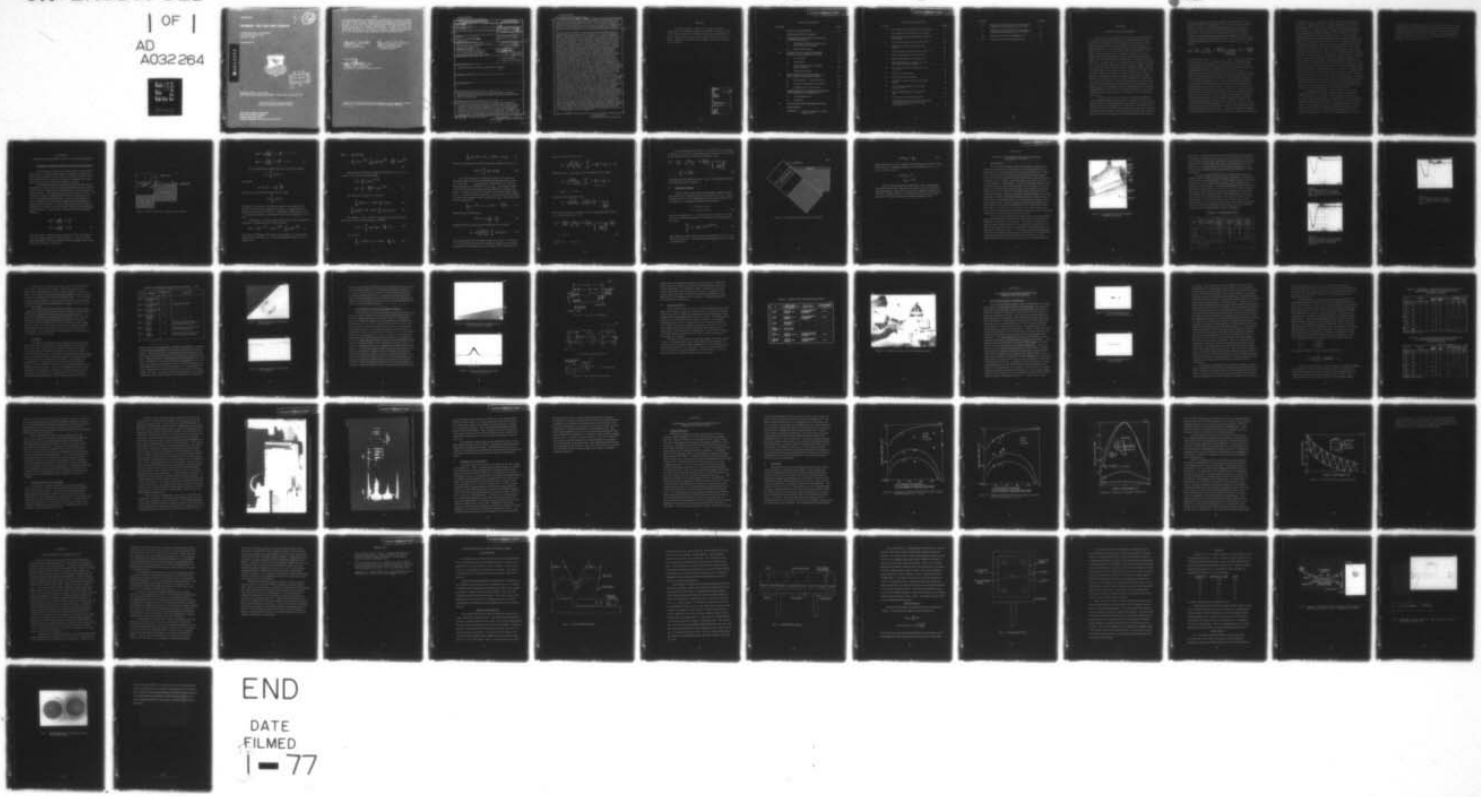

END

DATE
FILMED
1-77

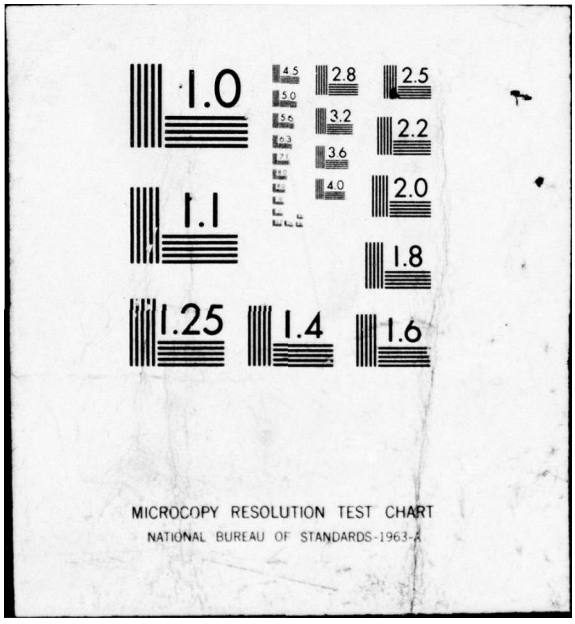
1.0
1.1
1.25
1.4
1.6
1.8
2.0
2.2
2.5
2.8
3.2
3.6
4.0
4.5
5.0
5.6
MICROCOPY RESOLUTION TEST CHART
NATIONAL BUREAU OF STANDARDS-1963-A

AFAL-TR-76-81

OPTIMIZED THIN FILM LIGHT SOURCES

HUGHES RESEARCH LABORATORIES
3011 MALIBU CANYON ROAD
MALIBU, CA 90265

SEPTEMBER 1976

TECHNICAL REPORT AFAL-TR-76-81
FINAL TECHNICAL REPORT FOR PERIOD 2 JANUARY 1975 - 2 JANUARY 1976

Approved for public release; distribution unlimited

AIR FORCE AVIONICS LABORATORY
AIR FORCE SYSTEMS COMMAND
UNITED STATES AIR FORCE
WRIGHT-PATTERSON AIR FORCE BASE, OHIO 45433

NOTICE

When Government drawings, specifications, or other data are used for any purpose other than in connection with a definitely related Government procurement operation, the United States Government thereby incurs no responsibility nor any obligation whatsoever; and the fact that the government may have formulated, furnished, or in any way supplied the said drawings, specifications, or other data, is not to be regarded by implication or otherwise as in any manner licensing the holder or any other person or corporation, or conveying any rights or permission to manufacture, use, or sell any patented invention that may in any way be related thereto.

Michael C. Hamilton

MICHAEL C. HAMILTON
Project Engineer/Physicist

Kenneth R. Hutchinson

KENNETH R. HUTCHINSON, Chief
Electro-Optics Techniques and
Applications Group

FOR THE COMMANDER

Jon C Zimmerman

ZIMMERMAN, JON C., MAJOR, USAF
Acting Chief, Electro-Optics Technology Branch

Copies of this report should not be returned unless return is required by security considerations, contractual obligations, or notice on a specific document.

AIR FORCE - 8 NOVEMBER 76 - 100

UNCLASSIFIED

SECURITY CLASSIFICATION OF THIS PAGE (When Data Entered)

REPORT DOCUMENTATION PAGE	READ INSTRUCTIONS BEFORE COMPLETING FORM
1. REPORT NUMBER: AFAL-TR-76-81	2. GOVT ACCESSION NO. / 3. RECIPIENT'S CATALOG NUMBER
4. TITLE (and Subtitle): OPTIMIZED THIN FILM LIGHT SOURCES	5. TYPE OF REPORT & PERIOD COVERED: Final Technical Report, 2 Jan 1975 - 2 Jan 1976 / 6. PERFORMING ORG. REPORT NUMBER
7. AUTHOR(s): Robert G. Hunsperger and Amnon Yariv	8. CONTRACT OR GRANT NUMBER(s): F33615-75-C-1024
9. PERFORMING ORGANIZATION NAME AND ADDRESS: Hughes Research Laboratories (DHO-2), 3011 Malibu Canyon Road, Malibu, CA 90265	10. PROGRAM ELEMENT, PROJECT, TASK AREA & WORK UNIT NUMBERS: Project No. 2001-02-31
11. CONTROLLING OFFICE NAME AND ADDRESS: Air Force Avionics Laboratory, Air Force Systems Command, Wright-Patterson AFB, Ohio 45433	12. REPORT DATE: September 1976 / 13. NUMBER OF PAGES: 55
14. MONITORING AGENCY NAME & ADDRESS (if different from Controlling Office)	15. SECURITY CLASS. (of this report): UNCLASSIFIED / 15a. DECLASSIFICATION DOWNGRADING SCHEDULE

16. DISTRIBUTION STATEMENT (of this Report)

Approved for public release; distribution unlimited

17. DISTRIBUTION STATEMENT (of the abstract entered in Block 20, if different from Report)

18. SUPPLEMENTARY NOTES

19. KEY WORDS (Continue on reverse side if necessary and identify by block number)

Hybrid Laser/Waveguide Source, Integrated Optics, Parallel End-Butt Coupling, Coupling Efficiency, (GaAl)As Injection Laser, Thin Film Waveguide

20. ABSTRACT (Continue on reverse side if necessary and identify by block number)

The objective of this program was to develop and demonstrate techniques for efficiently coupling a semiconductor injection laser source to a hybrid optical integrated circuit. The specific design objectives were to produce and deliver two hybrid coupled laser/waveguide sources in which the laser was operated at 300°K, driven with 20 to 250 nS length pulses at a repetition rate up to 10^4 P.P.S, emitting light at a wavelength between 0.8 μm into a thin film planar

next page

DD FORM 1 JAN 73 1473 EDITION OF 1 NOV 65 IS OBSOLETE

UNCLASSIFIED

SECURITY CLASSIFICATION OF THIS PAGE (When Data Entered)

micrometers

172 600

bpg

waveguide of either Ta_2O_5 or Nb_2O_5. At least one watt of peak optical power was to be coupled into the lowest order waveguide mode with a coupling efficiency of greater than 10%. All of the stated program objectives were achieved and in some cases surpassed. The approach used was to couple commerically available (GaAl)As laser diodes to thin film planar waveguides in a direct end-butt coupling arrangement.

The laser diodes used were single heterojunction (GaAl)As devices emitting peak pulse optical power as high as 24 W at a wavelength of 9040 Å. Standard production laser diodes were slightly modified to permit close coupling to the waveguides by omitting the usual cap and lens and by specially mounting the laser diodes to be flush with the edge of their heatsinks. The waveguides, supplied by the Air Force, were thin film planar guides of either Ta_2O_5 or 7059 glass on glass substrates. Waveguide thickness ranged from 1 to 2.5 μm. Calculations for the specific case of a (GaAl)As laser and Ta_2O_5 waveguide indicate that a coupling efficiency into the lowest order mode of approximately 90% is achievable for the ideal case of waveguide thickness equal to laser emitting layer thickness. Although we did not attain that ideal efficiency, the results we produced were in good agreement with theoretically predicted values for the laser and waveguide thicknesses that we used. The most difficult problem in the end butt coupling approach is how to accurately align the laser and waveguide to the close tolerances required without chipping the polished end faces of either the laser or waveguide. Theoretical and experimental results both indicated that control of the laser-waveguide spacing and the transverse lateral alignment of the laser and waveguide planes had to be within 0.1 μm in order to obtain optimum coupling. This problem was solved by using alignment fixtures driven by piezoelectrically adjusted micrometers with a resolution of 40 Å/V. The various tilt and rotational alignments were found to be much less critical then the spacing and lateral position, and were easily adjustable using a relatively simple mechanical stage. One of the two waveguide hybrids which was delivered combined a 2.0 μm Ta_2O_5 waveguide with a Laser Diode Labs type LD-67 laser diode. Peak optical power coupled into the lowest order mode was at least 2.39 W, corresponding to a coupling efficiency of 17% based on the optical power emitted from the waveguide. When corrections are made for waveguide attenuation of 2 dB/cm and output reflection loss of 11% the calculated value for coupled power is 6.44 W and the coupling efficiency into the lowest order mode is 45.1%. The second laser/waveguide hybrid which was delivered coupled an LD-67 laser to a 7059 glass waveguide that was 1.0 μm thick. The peak optical power coupled into the lowest order mode was 3.06 W at an efficiency of 11.3% in this case uncorrected for waveguide losses since the attenuation of the glass waveguide was not known accurately enough. This glass waveguide sample, which was fabricated by Rockwell International under separate contract to the Air Force, had an overlayed Ta_2O_5 thin film lens which was found to be effective in collimating the beam diverging from the laser at a FWHM angle of 30° to an angle of 8°.

PREFACE

This Final report was submitted by Hughes Research Laboratories, 3011 Malibu Canyon Road, Malibu, California 90265, under contract F33615-76-C-1024, job order number 20010231, with the Air Force Avionics Laboratory, Wright-Patterson AFB, Ohio 45433. Michael C. Hamilton, AFAL/DHO, is the Project Engineer for this project.

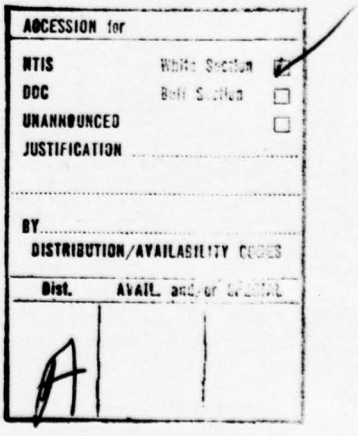

TABLE OF CONTENTS

LIST OF ILLUSTRATIONS

SECTION I

INTRODUCTION AND SUMMARY

The objective of this program was to develop and demonstrate techniques for efficiently coupling a semiconductor injection laser source to a hybrid optical integrated circuit. In particular, it was desired that an injection laser be coupled to a thin film Ta_2O_5 or Nb_2O_5 waveguide for eventual application in an acousto-optic RF spectrum analyzer of the type described by Hamilton and Wille.[1] The specific design objectives were to produce and deliver two hybrid coupled laser/waveguide sources in which the laser was operated at 300°K, driven with 20 to 250 nS length pulses at a repetition rate up to 10^4 P.P.S., emitting light at a wavelength between 0.8 μm and 1.0 μm into a thin film planar waveguide of either Ta_2O_5 or Nb_2O_5. At least one watt of peak optical power was to be coupled into the lowest order waveguide mode with a coupling efficiency of greater than 10%. All of the stated program objectives were achieved and in some cases surpassed. The approach used was to couple commercially available (GaAl)As laser diodes to thin film planar waveguides in a direct end-butt coupling arrangement. Critical alignment of the lasers and waveguides was accomplished using piezoelectrically driven stages. The aligned lasers and waveguides were then clamped together in specially designed fixtures to form a laser/waveguide hybrid unit. The results of this work have been summarized in a paper by R. G. Hunsperger and A. Lee.[2]

The laser diodes used were single heterojunction (GaAl)As devices emitting peak pulse optical power as high as 24 W at a wavelength of 9040 Å. Standard production laser diodes were slightly modified to permit close coupling to the waveguides by omitting the usual cap and lens and by specially mounting the laser diodes to be flush with the edge of their heatsinks. Measurements of the near field emission pattern of the lasers indicated an essentially Gaussian mode shape in

the direction normal to the junction plane with a full-width-at-half maximum (FWHM) of approximately 5 μm. The waveguides, supplied by the Air Force, were thin film planar guides of either Ta_2O_5 or 7059 glass on glass substrates. Waveguide thickness ranged from 1 to 2.5 μm. The ratio of waveguide thickness (t_g) to laser diode emitting layer thickness (t_L) is an important parameter for end butt coupling. The theoretical expression which was derived for the coupling coefficient $|A_S|^2$ (the fraction of laser power coupled into the S order mode) is

$$|A_S|^2 = \frac{64}{S^2\pi^2} \cdot \frac{n_L n_g}{(n_L + n_g)^2} \cdot \cos^2\left(\frac{\pi t_g}{2t_L}\right) \cdot \frac{1}{\left[1-\left(\frac{t_g}{St_L}\right)^2\right]^2} \cdot \frac{t_g}{t_L} \cdot \sin^2\left(\frac{S\pi}{2}\right),$$

where the mode number S = 1, 2, 3, 4..., and n_L and n_g are the indices of refraction of the laser and guide respectively. Calculations using this expression for the specific case of a (GaAl)As laser and Ta_2O_5 waveguide indicate that a coupling efficiency into the lowest order mode of approximately 90% is achievable for the ideal case of $t_g/t_L = 1$. Although we did not attain that ideal efficiency, the results we produced were in good agreement with theoretically predicted values for the laser and waveguide thicknesses that we used. The most difficult problem in the end butt coupling approach is how to accurately align the laser and waveguide to the close tolerances required without chipping the polished end faces of either the laser or waveguide. Theoretical and experimental results both indicated that control of the laser-waveguide spacing and the transverse lateral alignment of the laser and waveguide planes had to be within 0.1 μm in order to obtain optimum coupling. This problem was solved by using alignment fixtures driven by piezoelectrically adjusted micrometers with a resolution of 40 Å/V. The various tilt and rotational alignments were found to be much less critical than the spacing and lateral position, and were easily adjustable using a relatively simple mechanical stage. To facilitate alignment and subsequent bonding into a hybrid unit a laser/waveguide assembly was designed,

consisting of two basic components, a 5/8" diameter laser heatsink cylinder and a support structure in which the waveguide is secured by two clamping bars. The cylindrical laser heatsink fits into an oversized hole in the waveguide support structure in such a way that alignment adjustments are possible (angles $\leq 10^{o}$, translations ≤ 0.125"). Following alignment the laser heatsink cylinder and the waveguide support structure are clamped together by means of eight setscrews to form a hybrid unit which can be removed from the alignment stages and transported as desired. One of the two laser/waveguide hybrids which was delivered combined a 2.0 μm thick Ta_2O_5 waveguide with a Laser Diode Labs type LD-67 laser diode. Peak optical power coupled into the lowest order mode was at least 2.39 W, corresponding to a coupling efficiency of 17%, based on the optical power emitted from the waveguide. When corrections are made for waveguide attenuation of 2 dB/cm and output reflection loss of 11% the calculated value for coupled power is 6.44 W and the coupling efficiency into the lowest order mode is 45.1%. The second laser/waveguide hybrid which was delivered coupled an LD-67 laser to a 7059 glass waveguide that was 1.0 μm thick. The peak optical power coupled into the lowest order mode was 3.06 W at an efficiency of 11.3%, in this case uncorrected for waveguide losses since the attenuation of the glass waveguide was not known accurately enough. This glass waveguide sample, which was fabricated by Rockwell International under separate contract to the Air Force, had an overlayed Ta_2O_5 thin film lens which was found to be effective in collimating the beam diverging from the laser at a FWHM angle of 30^{o} to an angle of 8^{o}.

The principal limit to the coupling efficiency with the butt coupling method is the thickness mismatch between the laser light emitting layer and the waveguide, characterized by the ratio t_g/t_L. By using a double heterostructure cw (GaAl)As injection laser with an emitting layer thickness = 0.25 μm the ratio t_g/t_L can be improved by a factor of 20 compared to that for the pulsed laser diodes. Such cw lasers became available toward the end of this program and we did investigate coupling one to a 7059 glass waveguide. However we achieved a coupled power of only 0.74 W (10% efficiency) because the

laser diode was not flush with the edge of the heatsink, preventing close coupling of the laser and waveguide. The need for the laser to be flush mounted or protruding on the heatsink presents a particular problem in the case of present day cw lasers which require extremely good heat-sinking. As improvements in laser and heatsink design are made this problem will become less significant.

SECTION II

THEORETICAL ANALYSIS OF THE BUTT COUPLING PROBLEM

A. Derivation of Coupling Coefficients for Parallel Butt Coupling

In what follows we will derive an expression for the fraction of power that can be coupled from a large waveguide to a smaller waveguide by butt coupling as shown in Fig. 1. Practical situations where this problem may be of interest to include the coupling from a large optical cavity laser to a thin film modulator waveguide.

The approach consists of expanding the fields on both sides of the butt joint in terms of the respective waveguide modes and requiring continuity across the interface of the tangential electric and magnetic field components. The analysis will be carried out for a TE wave. The results are expected to hold also for TM waves if operation is well above the propagation cutoff condition. Since we are interested in power exchange between modes the problem of mode normalization requires careful attention. A general formulation of these modes is unnecessarily complicated for our purpose. In the case of propagation well above cutoff, we can take the y component of the fundamental modes as

$$\mathcal{E}_g(x) = 2\sqrt{\frac{\omega\mu}{\beta_g t_g}} \cos \frac{\pi x}{t_g}$$

$$\mathcal{E}_L(x) = 2\sqrt{\frac{\omega\mu}{\beta_L t_L}} \cos \frac{\pi x}{t_L} \qquad (1)$$

where the g and L subscripts refer respectively to the waveguide and laser with heights t_g and t_L as shown in Fig. 1. In the case of the output waveguide we will also need the form of the higher order modes which may be excited. These are[3]

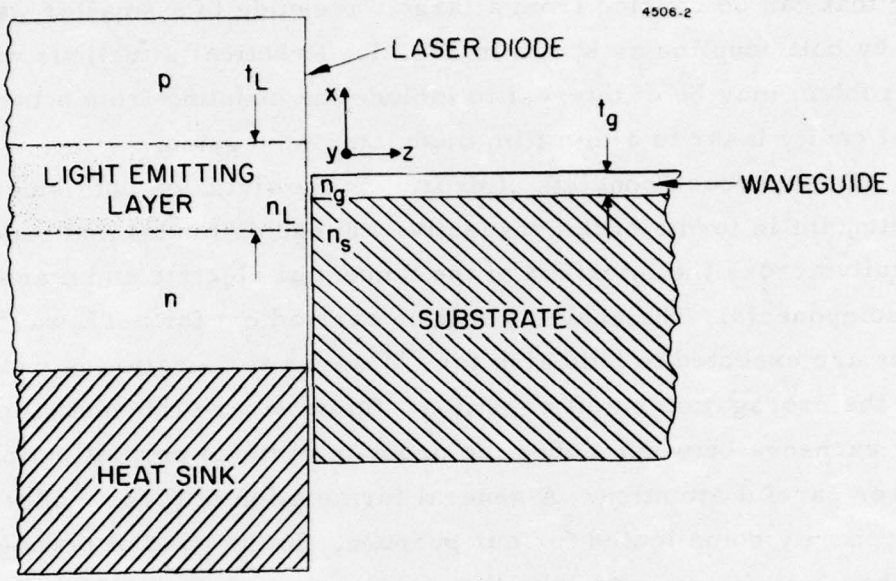

Figure 1. Butt coupled laser collinear with waveguide.

$$\mathscr{E}_{gS}(x) = 2\sqrt{\frac{\omega\mu}{\beta_{gS}t_g}} \cos \frac{\pi x S}{t_g} , \quad S = 1, 3, 5 \ldots$$

$$\mathscr{E}_{gS}(x) = 2\sqrt{\frac{\omega\mu}{\beta_{gS}t_g}} \sin \frac{\pi x S}{t_g} , \quad S = 2, 4 \ldots \quad . \qquad (2)$$

The normalization constants of (2) are such that the integral

$$-\frac{1}{2}\int_{-\infty}^{\infty} E_y H_x^* \, dx = 1$$

if the fields

$$E_y \text{ and } H_x = -\frac{i}{\omega\mu_o}\frac{\partial \mathscr{E}_y}{\partial z}$$

are taken as the mode fields as given by (2). Since

$$-\frac{1}{2}\int_{-\infty}^{\infty} E_y H_x^* \, dx$$

corresponds to the power carried by the mode for unit width in the y direction, it follows that a mode with a field $E_y = A\,\mathscr{E}_{gS}(x)$ carries an amount of power equal to $|A|^2$ W/m. Returning to the problem at hand, let us assume that field is incident from the left on the interface $z = 0$ of Fig. 1.

The field at $z < 0$ will be taken as that of the incident fundamental mode plus a summation over the reflected modes

$$\overline{\mathscr{E}}_y(x) = \overline{\mathscr{E}}_o(x)\, e^{-i\beta_o z} + r_o \overline{\mathscr{E}}_o(x)\, e^{i\overline{\beta}_o z} + \sum_{k \neq 0} r_k \overline{\mathscr{E}}_k(x) e^{i\overline{\beta}_k z} \quad . \qquad (3)$$

The incident field $\overline{\mathscr{E}}_o(x)$ is taken with a unity amplitude. The reflection coefficient into mode $\overline{\mathscr{E}}_k$ is r_k. The incident magnetic field at $z < 0$ is obtained from

$$\bar{\mathcal{H}}_y(x) = -\frac{i}{\omega\mu_o}\frac{\partial}{\partial z}\bar{\mathcal{E}}_y(x)$$

$$= -\frac{\bar{\beta}}{\omega\mu_o}\bar{\mathcal{E}}_o(x)\, e^{-i\bar{\beta}_o z} + \sum_{k\neq 0} r_k\bar{\beta}_k\bar{\mathcal{E}}_k(x)e^{i\bar{\beta}_k z} + \frac{r_o\beta_o}{\omega\mu_o}\bar{\mathcal{E}}_o(x)e^{i\bar{\beta}_o z} \quad . \tag{4}$$

The transmitted field to the right of the interface (i.e., at $z > 0$) is taken as a sum over the normal modes

$$\mathcal{E}_y(x) = \sum_m A_m\mathcal{E}_m(x)\, e^{-i\beta_m z}$$

$$\mathcal{H}_y(x) = \sum_m -\frac{\beta_m A_m}{\omega\mu_o}\mathcal{E}_m(x)e^{-i\beta_m z} \quad . \tag{5}$$

The continuity of $\mathcal{E}_y(x)$ at $z = 0$ leads to

$$\sum_{k\neq 0} r_k\bar{\mathcal{E}}_k(x) + (r+1)\bar{\mathcal{E}}(x) = \sum_m A_m\mathcal{E}_m(x) \tag{6}$$

$$\sum_{k\neq 0} \bar{\beta}_k r_k\bar{\mathcal{E}}_k(x) + \bar{\beta}(r-1)\bar{\mathcal{E}}(x) = \sum_m -\beta_m A_m\mathcal{E}_m(x) \quad . \tag{7}$$

We multiply, in turn, (6) and (7) by $\mathcal{E}_S(x)$ and integrate over the cross section using the orthonormality condition[3]

$$\langle m/S\rangle \equiv \int_{-\infty}^{\infty}\mathcal{E}_m(x)\,\mathcal{E}_S(x) = \frac{2\omega\mu}{\beta_S}\delta_{S,m} \quad . \tag{7a}$$

The result is

$$\sum_{k\neq 0} r_k\langle\bar{k}|S\rangle + (r_o+1)\langle\bar{0}|S\rangle = \frac{2\omega\mu}{\beta_S}A_S \tag{8}$$

$$\sum_{k\neq 0} r_k \overline{\beta}_k \langle \overline{k} | S \rangle + \overline{\beta}(r_o - 1) \langle \overline{0} | S \rangle = - 2\omega\mu A_S \qquad (9)$$

where we are using the top bar to indicate the mode function at $z < 0$

$$\langle \overline{k} | S \rangle \equiv \int_{-\infty}^{\infty} \overline{\mathscr{E}}_k(x)\ \mathscr{E}_S(x) dx \ . \qquad (10)$$

Our prime interest is in solving for $|A_S|^2$, the fraction of the power coupled from the fundamental mode incident from the left ($z < 0$) into the waveguide mode to the right ($z > 0$). The unknowns appearing in (8) and (9) are r_k and A_S. The equations cannot be solved in their present form since the number of variables is too large. A solution for A_S can be obtained if we assume that $\overline{\beta}_k = \overline{\beta}_o$ for all k i.e., neglect the mode dispersion. This is nearly true for model well above the propagation cutoff where $\overline{\beta}_k \cong (\omega/c) n_L$. With this assumption we rewrite (9) as

$$\sum_{k\neq 0} r_k \langle k | S \rangle + (r_o - 1) \langle 0 | S \rangle = - \frac{2\omega\mu A_S}{\beta} \ . \qquad (11)$$

Subtracting (11) from (8) gives

$$\langle 0 | S \rangle = \omega\mu A_s \left(\frac{1}{\beta_S} + \frac{1}{\overline{\beta}} \right) \ . \qquad (12)$$

Solving (12) for A_S and using the definition in eq. (7a) yields

$$A_S = \frac{1}{\omega\mu} \left(\frac{\overline{\beta}_o \beta_S}{\overline{\beta}_o + \beta_S} \right) \int_{-\infty}^{\infty} \overline{\mathscr{E}}_o(x)\, \mathscr{E}_S(x)\, dx \ . \qquad (13)$$

The coupling coefficient into mode S is given by $|A_S|^2$. To evaluate it we need to know the mode functions $\overline{\mathscr{E}}_o(x)$ and $\mathscr{E}_S(x)$ as well as their propagation constants $\overline{\beta}_o$ and β_S. In the limit of well confined modes

we use eq. (2) to write eq. (13) as

$$A_S = \frac{4\bar{\beta}_o^{1/2}\,\beta_S^{1/2}}{(\bar{\beta}_o + \beta_S)\sqrt{t_g t_L}} \int_{-t_g/2}^{t_g/2} \cos\frac{\pi x S}{t_g} \cos\frac{\pi x}{t_L}\, dx \qquad (14)$$

using $\beta_o \approx (\omega/c)n_L$, $\beta_S \approx (\omega/c)n_S$ in the prefactor of (14) we obtain

$$A_S \approx \frac{4\sqrt{n_L n_S}}{(n_L + n_S)\sqrt{t_g t_L}} \int_{-t_g/2}^{t_g/2} \cos\frac{\pi x S}{t_g} \cos\frac{\pi x}{t_L}\, dx \qquad S = 1, 3, 5 \ldots .$$

$$A_S \cong 0 \qquad S = 2, 4, \ldots$$

Carrying out the integration yields

$$A_S = \frac{8\sqrt{n_L n_S}}{\pi S(n_L + n_S)} \cos\left(\frac{\pi t_g}{2t_L}\right) \sqrt{\frac{t_g}{t_L}}\, \frac{1}{1 - \left(\frac{t_g}{St_L}\right)^2} .$$

The fraction of the power coupled from the fundamental mode $\mathcal{E}_o(x)$ at $z < 0$ into the mode S at $z > 0$ is

$$|A_S|^2 = \left(\frac{8}{\pi S}\right)^2 \frac{n_L n_S}{(n_L + n_S)^2} \cos^2\left(\frac{\pi t_g}{2t_L}\right) \frac{1}{\left[1 - \left(\frac{t_g}{St_L}\right)^2\right]^2} \left(\frac{t_g}{t_L}\right)$$

$$S = 1, 3, 5 \ldots \qquad (15)$$

$$|A_S|^2 \cong 0 \qquad S = 2, 4, \ldots .$$

For waveguide modes far above cutoff little error is introduced by taking $n_S \simeq n_g$, and also the dissappearance of the even order modes can be concisely stated by including a factor $\sin^2 S\pi/2$.

$$|A_S|^2 = \frac{64}{S^2\pi^2} \cdot \frac{n_L n_g}{(n_L + n_g)^2} \cdot \cos^2\left(\frac{\pi t_g}{2t_L}\right) \cdot \frac{1}{\left[1 - \left(\frac{t_g}{St_L}\right)^2\right]^2}$$

$$\cdot \frac{t_g}{t_L} \sin^2\left(\frac{S\pi}{2}\right) . \qquad (15a)$$

A comparison of calculated values for $|A_S|^2$ with experimentally measured results is given in Section V.

B. Angle Butt Coupling

Here we consider the effect on the coupling coefficient $|A_S|^2$ of having the two waveguides tilted by an angle ϕ as in Fig. 2. Such a situation may arise if the butting plane are not exactly normal to the waveguide axes. Using the coordinate transformation

$$z' = z\cos\phi - x\sin\phi$$
$$x' = z\sin\phi + x\cos\phi \qquad (16)$$

now on the butting plane $z' = 0$ so from eq. (16) we have $z = x\tan\phi$. The result of this transformation is to change the overlap integral in eq. (13) to

$$\int_{-t_g/2}^{t_g/2} \bar{\mathscr{E}}_o \frac{x}{\cos\phi} \mathscr{E}_S(x) e^{i\beta_S x\tan\phi} dx . \qquad (17)$$

This integral is always smaller than its counterpart in eq. (13). The difference, however, is not appreciable until $(\beta_S t_g/2)\tan\phi \approx \pi$ which can be written as

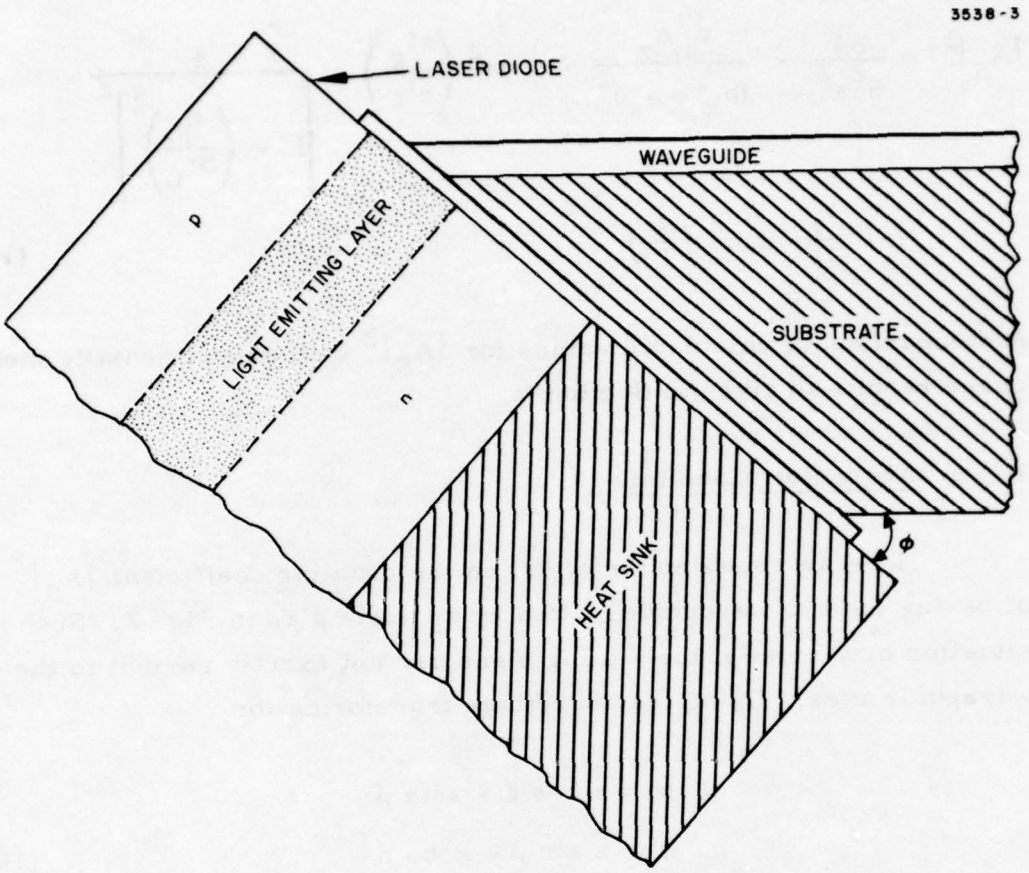

Figure 2. Butt coupled laser angled with waveguide.

$$(\tan \phi)_{max} \approx \frac{\lambda}{nt_g} \quad . \tag{18}$$

Equation (18) can be used to estimate the limiting angle at which we may expect decrease of coupling efficiency. As an example for $n \approx 3$, $\lambda = 1$ μm, $t_g = 2$ μm, we have

$$(\tan \phi)_{max} \approx 1/6$$

$$\phi_{max} = 9.46^{\circ}$$

Thus we see that angle butt coupling has a lower coupling efficiency than parallel butt coupling for all angles and is not a preferred coupling technique. However, the tolerance to angular misalignment is such that a minimal decrease in coupling efficiency occurs for angles less than $\simeq 9^{\circ}$ when the parallel butt coupling technique is used.

SECTION III

DESIGN OF THE LASER/WAVEGUIDE HYBRID AND ALIGNMENT FIXTURES

A. Laser Diodes

Commercially available, single heterojunction, pulsed laser diodes were used because suitable devices emitting greater than 20 W peak pulse power could be obtained for less than $50.00 each. Diodes were ordered without the usual cap and lens to permit butt coupling. We tested four types of diodes with the manufacturer's specified characteristics, shown in Table 1. All of the diodes were found to conform to the manufacturer's specifications. In order to obtain the required close coupling between the laser and waveguide it was necessary to have the laser diode positioned flush with the edge of the heatsink or protruding slightly over the edge so that the heatsink would not interfere with the waveguide substrate. Since the standard production diodes are generally mounted on a slightly oversized molybdenum pellet, as shown in Fig. 3 (to facilitate prepackaging testing), it was necessary to order specially flush mounted diodes. Since the range of typical peak emitted power for the 400 μm wide diodes overlapped that of the 600 μm wide diodes (see Table 1), we decided to use the 400 μm wide LD-67 diodes which have a lower threshold current and larger duty factor but can be specially selected to have peak emitted power of 20 to 25 W.

One of the LD-69 diodes was examined by means of the scanning-electron-microscope and electron-beam-microprobe to determine the thickness of the light generating layer. This diode is a single heterojunction confined field type which has a p-type light emitting layer of GaAs on an n-type GaAs substrate capped with a p-type (GaAl)As confining layer, as shown in Fig. 3. The measurements indicated that the thickness of the light generating layer, bounded on top by the (GaAl)As-GaAs heterojunction and on bottom by the p-n junction, is 2.0 μm. Optical measurements of the near-field pattern of the diode (operated

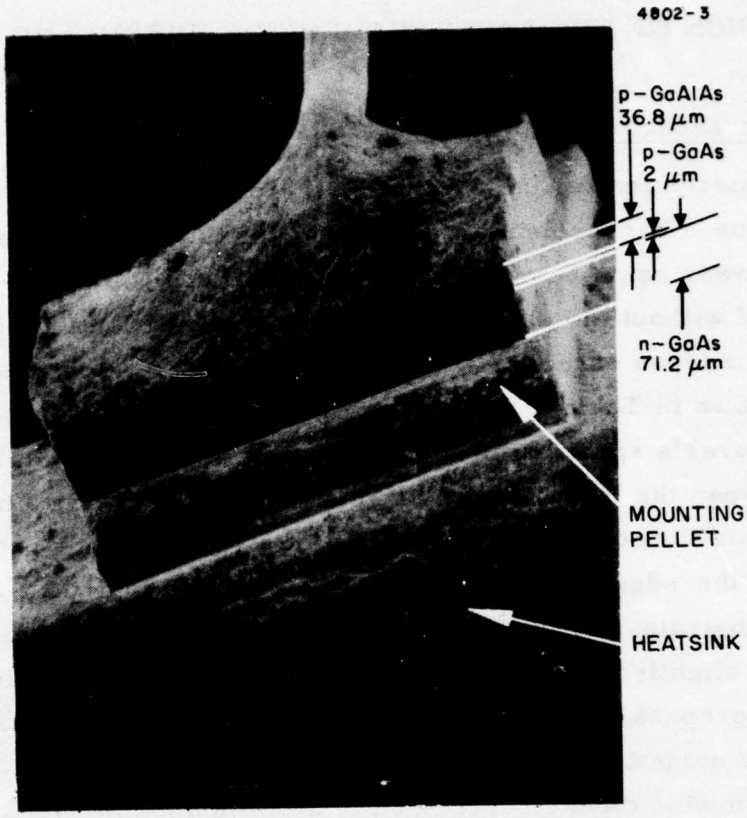

Figure 3. Scanning-electron-micrograph of (GaAl)As laser diode.

with a dc I_f = 100 mA) indicated an essentially Gaussian mode shape in the direction normal to the junction plane with a full width at half maximum of approximately 5 μm. Spreading of the light from the generating layer is to be expected since this is only a single heterojunction laser and there is no confining layer on one side of the p-n junction. The effect of this spreading on the coupling efficiency is discussed in detail in Section V.

The lasers were mounted on 1.5 in. long 5/8 in. in diameter copper heatsink cylinders, and were driven by means of a Laser Diode Laboratories type LP-210 pulser. With the pulser and laser diode interconnected by a 6 in. length of coaxial cable a clean current pulse is obtained as shown in Fig. 4. The emitted light pulse closely follows the shape of the current pulse, as can be seen in Fig. 5. As the length of the coaxial cable is increased the pulse shape degrades, increasing in both risetime and total pulse length. This degradation can be seen in Fig. 6 which shows the pulse shape for the case of a 48-in. interconnecting cable. The slower risetime reduces overall laser diode efficiency because a greater percentage of the pulse length is composed of current below the threshold level for lasing. Thus it is advisable to keep the interconnecting cable as short as possible.

TABLE 1. LASER DIODE DATA

Diode Type	Maximum Peak Forward Current A	Typical Threshold Current, A	Emitting Area Dimensions, Width x Thickness, μm	Wavelength of Peak Intensity, A	Maximum Pulse Length for 10^4 pps rate nsec	Peak Emitted Power at Maximum Current W
LD-67	75	16	400 x 2	9040	100	15 to 25
LD-69	100	30	600 x 2	9040	60	25 to 30
SG2010	75	25	400 x 2	9040	100	15 to 20
SG2012	100	36	600 x 2	9040	50	20 to 25

Note: Type LD = Laser Diode Laboratories
Type SG = RCA

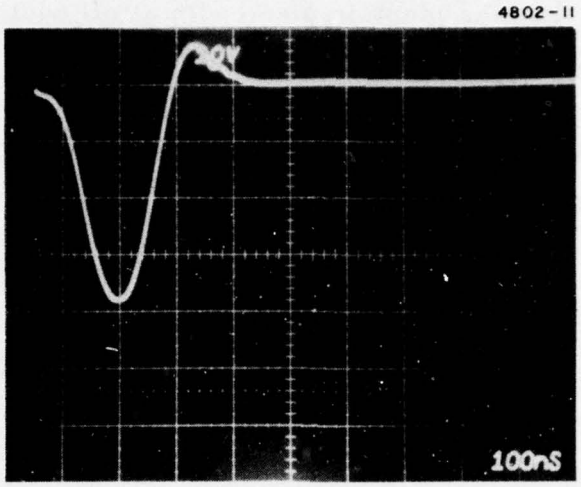

Figure 4.
Current pulse driving laser diode LD67-7 (through a 6-in. length of coax). Vertical 20 A/div; horizontal 100 ns/div.

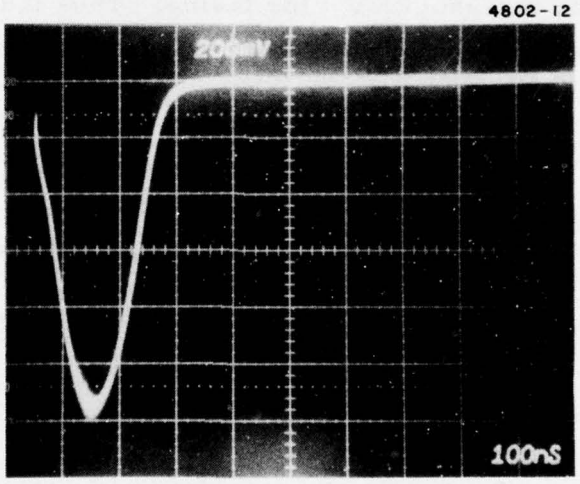

Figure 5.
Light pulse emitted from laser diode LD67-7 (coupled to waveguide DC-1). Vertical 0.4 W/div; horizontal 100 ns/div.

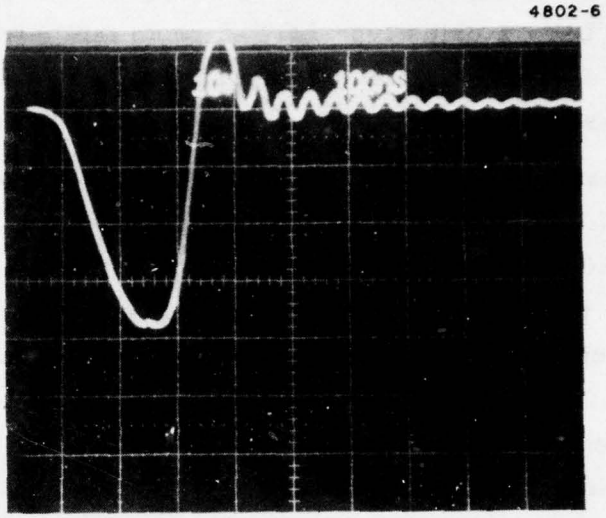

Figure 6.
Current pulse driving laser diode LD67-7 (through a 48-in. length of wax). Vertical 20 A/div; horizontal 100 ns/div.

In addition to the pulsed laser diodes, which were used in most of the work, we also performed some coupling experiments with a Laser Diode Laboratories type LCW-5 room temperature, cw laser diode. This device is a double heterostructure type laser with a nominal emitting layer thickness of 0.25 μm and width of 12 μm. The wavelength of peak emission is 8900 A. The particular laser used had a threshold current of 270 mA and a maximum emitted cw power of 8.9 mW at a dc current of 320 mA.

Since polarization of the emitted laser light will strongly affect coupling efficiency into a particular mode, we measured the polarization of the output from some laser diodes by using a prism polarizer. As expected, the light was strongly polarized with the E vector transverse to the direction of emission and parallel to the plane of the junction. For LD-67 and LD-69 (pulsed) laser diodes operated near peak output power the ratio of the transmitted intensity with the polarizer oriented perpendicular to the junction plane to that with it oriented parallel was $\simeq 0.0006$. For a type LCW-5 room temperature cw laser diode the corresponding ratio was $\simeq 0.001$.

B. Waveguides

Two types of waveguides, Ta_2O_5 and glass waveguides both on glass microscope slide substrates, were supplied by the Air Force for use in this work. Table 2 gives a summary of the features of these waveguides and lists the assigned labels that we will use to identify them throughout this report. To prepare the waveguides for butt coupling they were scribed and broken to produce samples of various lengths and the end faces were dressed to 90° and polished. The polishing was accomplished by a tedious but effective hand lapping and finishing process. Alumina abrasive was used for rough lapping followed by fine polishing with cerium oxide. To prevent rounding of the critical waveguide edge, the sample to be polished was sandwiched between microscope slides waxed together. A lapping fixture was used to hold the waveguide sample perpendicular to the polishing plate containing the

TABLE 2. WAVEGUIDE DESIGNATION AND DESCRIPTION

Label	Material	Thickness, μm	Comments
DC-1	DC Sputtered Ta_2O_5	2.0	
DC-2	DC Sputtered Ta_2O_5	1.0	2 samples provided
RF-1	RF Sputtered Ta_2O_5	1.7	
BA-1	Barium Silicate Glass	0.5	
R-1	7059 Glass	1.0	Included Ta_2O_5 thin film lens with double convex shape
R-2	7059 Glass	1.0	Included Ta_2O_5 thin film lens with round spot shape
R-3	7059 Glass	2.5	Included Ta_2O_5 thin film lens with double convex shape

abrasive slurry. During polishing, samples were repeatedly examined by 1000X optical microscopy to evaluate the condition of the polished surface. After polishing they were examined in the scanning electron microscope to check the final polish and to determine waveguide thickness. Figures 7 and 8 are optical photographs of waveguides DC-1 and DC-2, respectively. It can be seen that the waveguide edge on the air side is not rounded and that glitches in the surface polish take up less than 10% of the total area of the waveguide face. It was possible to locate regions where no significant defects were visible over lateral lengths of 100 μm. The thickness of the waveguides can be accurately determined in the scanning electron microscope either by observing

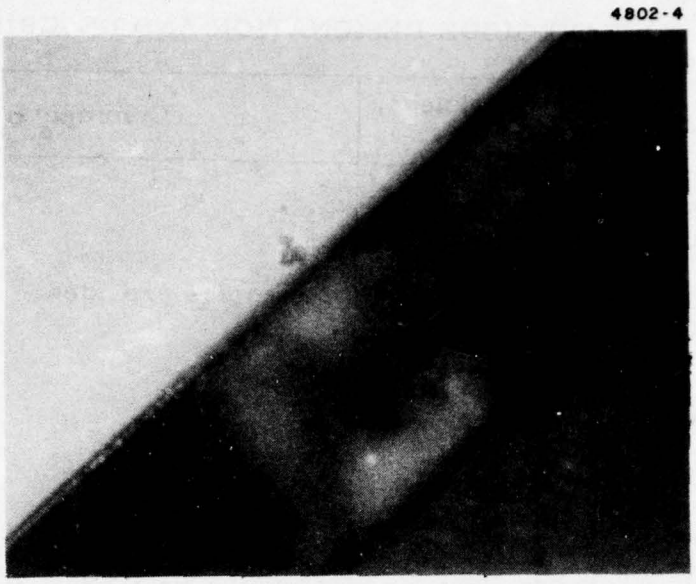

Figure 7. Optical photograph of waveguide DC-1 (1000X).

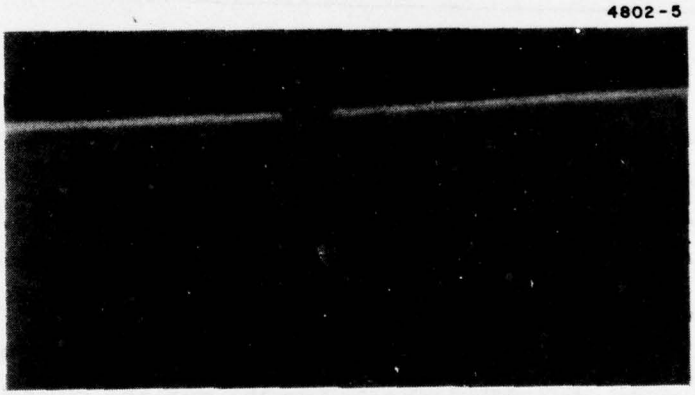

Figure 8. Optical photograph of waveguide DC-2 (1000X).

the image generated by secondary electron emission as in Fig. 9 which clearly shows a bright line at the waveguide-substrate interface, or by making an x-ray rate scan to detect x rays emitted by one of the waveguide constitutent elements. A typical rate scan for the TaL $_{\alpha}$ line emitted from waveguide DC-1 is shown in Fig. 10. By using the SEM in both the secondary electron and x-ray emission modes one has a dual check on waveguide thickness.

C. Laser Heatsink and Waveguide Support Structure

The hybrid laser/waveguide assembly consists of two basic components, a 5/8 in. diameter laser heatsink cylinder shown in Fig. 11 and a waveguide support structure shown in Fig. 12. The heatsink cylinder is drilled and tapped to accept either the Laser Diode Labs or RCA lasers on one end, and a standard BNC fitting on the other end. The waveguide is held in its support structure by two clamping bars. A modification made to the waveguide support structure during the optimization phase of the program was to add two 1/16 in. thick Teflon pads under the clamping bars to prevent chipping or cracking of the waveguide. The cylindrical laser heatsink fits into an oversized hole in the waveguide support structure in such a way that alignment adjustments are possible (angles $\leq 10^{\circ}$, translations ≤ 0.125 in.) prior to setscrew clamping and/or epoxy bonding of the heatsink and waveguide support. In the initial design the eight setscrews were intended to provide only preliminary clamping until epoxy bonding of the heatsink cylinder and waveguide support could be accomplished by filling the space between them with epoxy; however, the setscrew clamping alone was found to produce reliable bonding between laser and waveguide sufficient to maintain optimum alignment during normal handling and transport. Hence the epoxy filler was not used in the laser/waveguide

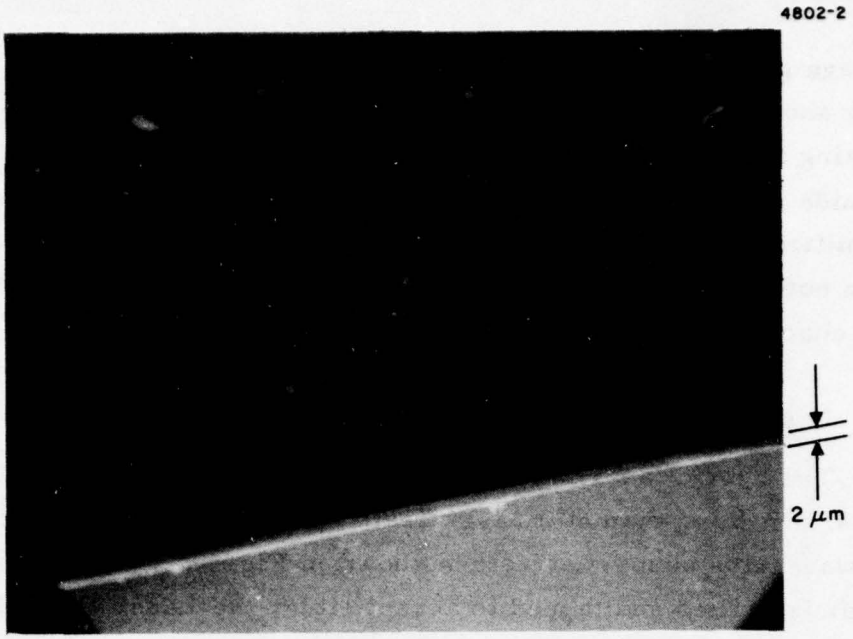

Figure 9. SEM photograph of waveguide DC-1 by secondary electron emission.

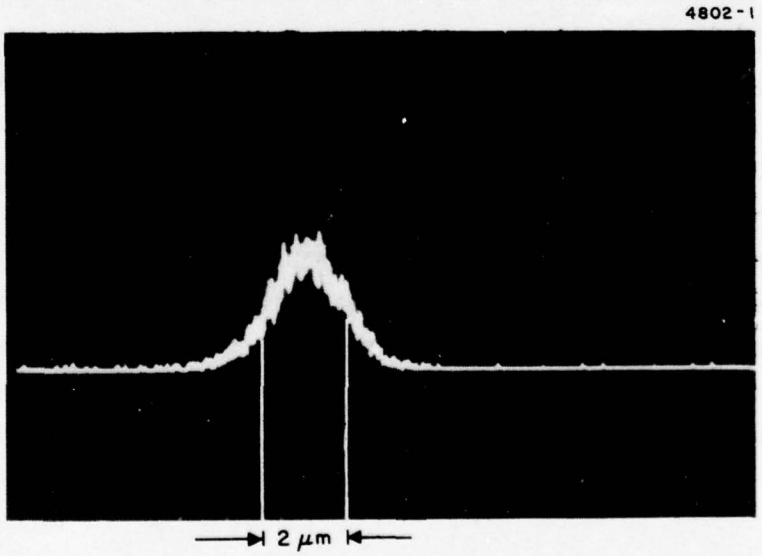

Figure 10. X-ray rate scan of waveguide DC-1 for $T_a L_a$ line.

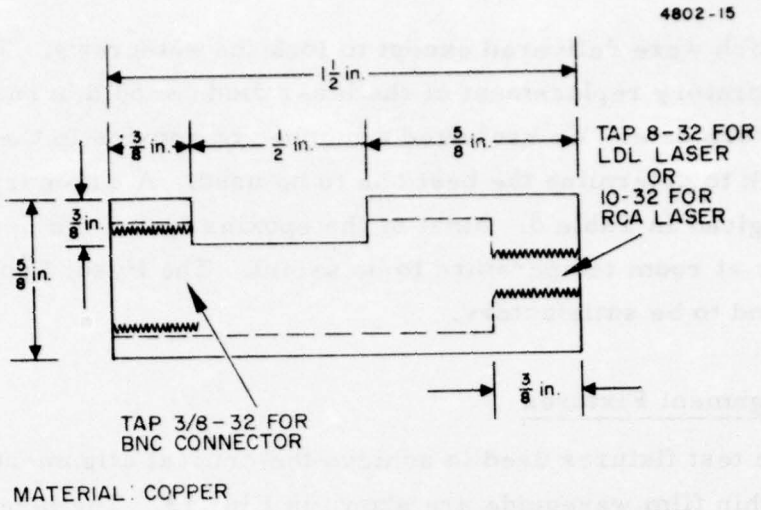

Figure 11. Laser heatsink drawing.

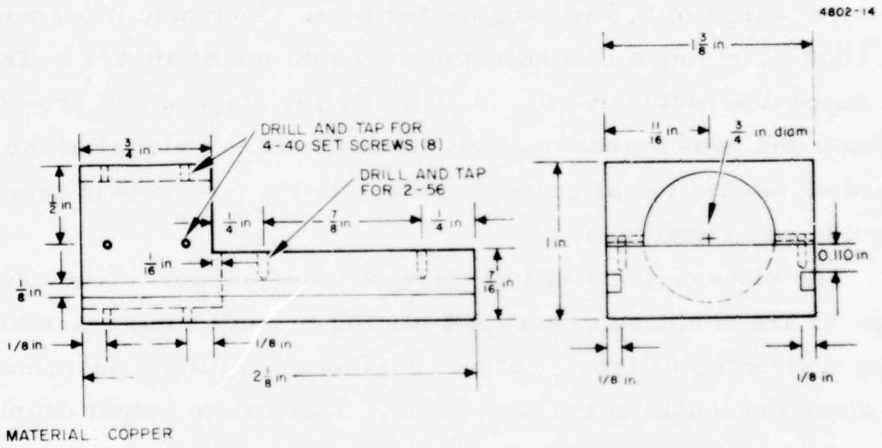

a. Waveguide support structure.

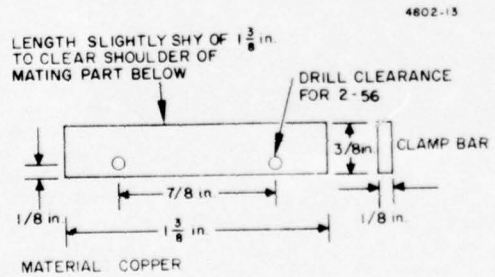

b. Clamping bars.

Figure 12. Waveguide holder drawings.

hybrids which were delivered except to lock the setscrews. This will permit laboratory replacement of the laser diode should burnout occur at some future date. We evaluated a number of epoxies in the course of this work to determine the best one to be used. A summary of the results is given in Table 3. Most of the epoxies tested did not harden sufficiently at room temperature to be useful. The Hysol Epoxy-Patch 1C was found to be satisfactory.

D. Alignment Fixtures

The test fixtures used to achieve the critical alignment of the laser diode and thin film waveguide are shown in Fig. 13. The laser heatsink cylinder was held on a Jodon high resolution x-y-z micropositioner stage equipped with Tropel PZM electromicrometer drives. The PZM micrometers are mechanical/piezoelectric devices which have a mechanical adjustment range of 0.5 in. augmented by an electronic movement of 4 μm/1000 V, giving a fine adjustment resolution of 40 Å/V. The waveguide support structure was held on an Ealing stage which provided rotational and two-dimensional tilt adjustments. Thus all of the degrees of freedom needed for alignment of the relative positions of laser and waveguide were available.

The slots on the sides of the waveguide support structure, visible in Fig. 13 are designed to accept a sliding prism clamp assembly permitting a strontium titanate output coupling prism to be positioned at any point along the length of the waveguide. This prism output coupler was used to determine the modal distribution of optical power in the waveguide as well as to measure attenuation in the waveguide.

TABLE 3. RESULTS OF EPOXY EVALUATIONS

4716-3

NO.	TYPE	OBSERVED ROOM TEMPERATURE CURING TIME AND HARDNESS	EFFECT OF 48 h TREATMENT AT 50° C	LINEAR EXPANSION AFTER HEAT TREATMENT $\lvert \Delta \ell / \ell \rvert$
1	EPO-TEK 305	SETS IN 16 h 4 DAYS FOR PLASTIC HARDNESS	NO LOSS OF ADHERENCE NO IMPROVEMENT IN HARDNESS	$< 4 \times 10^{-4}$
2	EPO-TEK 310	SET IN 16 h 4 DAYS FOR PLASTIC HARDNESS	NO LOSS OF ADHERENCE NO IMPROVEMENT IN HARDNESS	$< 8 \times 10^{-4}$
3	EPO-TEK 320	STILL HAS TAR-LIKE CONSISTENCY AFTER 20 DAYS	—	—
4	FREY ENGINEERING CF-3009	SET IN 3 min, BUT REMAINS GUMMY	—	—
5	HYSOL EPOXI-PATCH 1C	SET IN 2 h 2 DAYS FOR GLASS-LIKE HARDNESS	NO LOSS OF ADHERENCE. NO OBSERVABLE CHANGE IN HARDNESS	$< 6 \times 10^{-4}$
6	SUMMERS LENS BOND M62	SETS IN 16 h 5 DAYS FOR PLASTIC HARDNESS	NO LOSS OF ADHERENCE NO IMPROVEMENT IN HARDNESS	$< 6 \times 10^{-4}$

M11279

5802-16

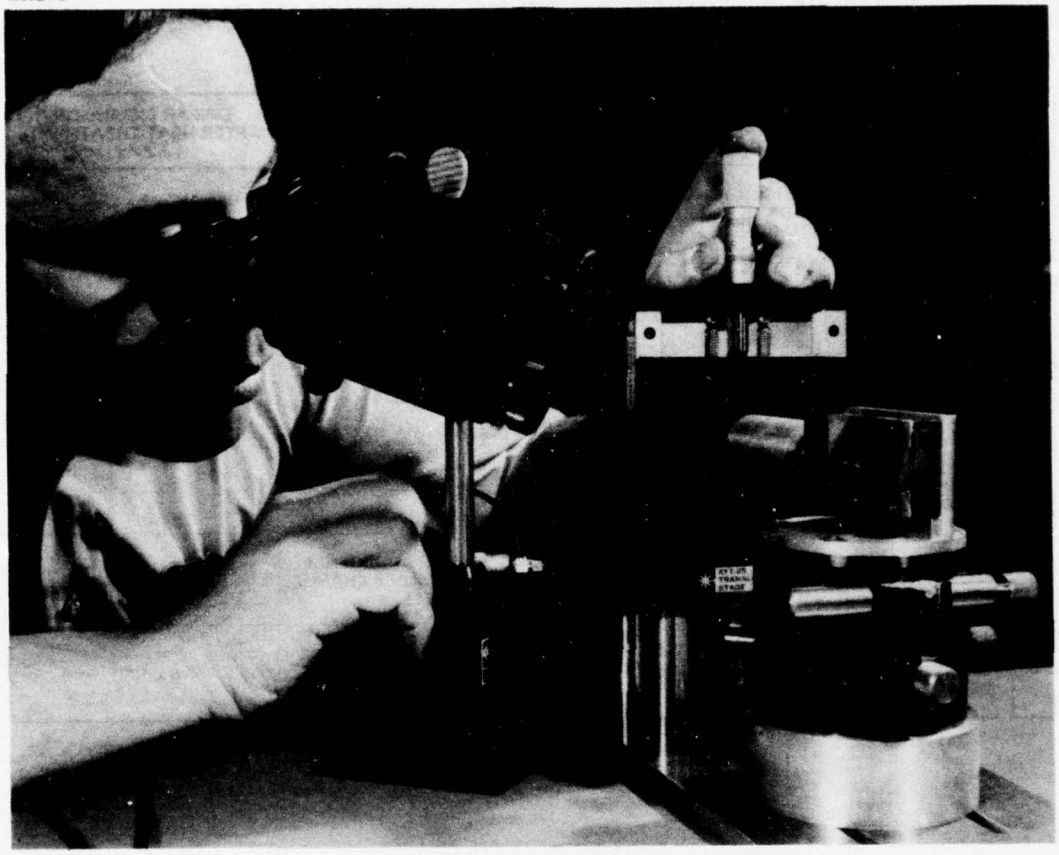

Figure 13. Alignment fixtures and laser/waveguide hybrid.

SECTION IV

EVALUATION AND OPTIMIZATION OF THE LASER/WAVEGUIDE HYBRIDS

A. Butt Coupling – Power and Efficiency

The alignment fixtures shown in Fig. 13 were used to butt couple many different combinations of lasers and waveguides. In all cases a calibrated Si photodiode was used to measure the peak output power of the laser and the peak output power emitted from the end of the waveguide when coupled to the laser. The overall transmission efficiency (including lumped waveguide loss and input/output coupling loss) could thus be determined. Rough alignment was performed while observing the image of the waveguided light focused onto an image upconverter tube by means of a microscope objective. Final alignment was done by adjusting for maximum measured power. Figure 14 shows the image of the light emitting layer of an LD-69 type laser diode, while Fig. 15 shows the light emitted from waveguide DC-1 when coupled to that same laser. The waveguided light is seen to be well confined, with a negligible background of unguided light traveling in the substrate. Note that the thickness of the layer of waveguided light appears to be only about 1/3 the thickness of the laser light emitting layer. This is consistent with the thickness measurements of 2.0 μm for the waveguide and ≃5 μm for the laser as described in Section III. The polarization of the light transmitted by the waveguide was measured with a prism polarizer and found to be totally TE. No TM component was observable. This result was expected since the laser was operating in the TE mode as described in Section III. In addition to the measurement of overall transmitted power we also determined the modal distribution of the power in the waveguide for most samples. This was done by clamping a strontium titanate prism to the waveguide to act as an output coupler. Light was thus coupled out of the waveguides in a pattern of "m-lines" at different angles corresponding to the S = 1, 3 and (in some cases)

Figure 14. Near field photograph of laser diode light emission.

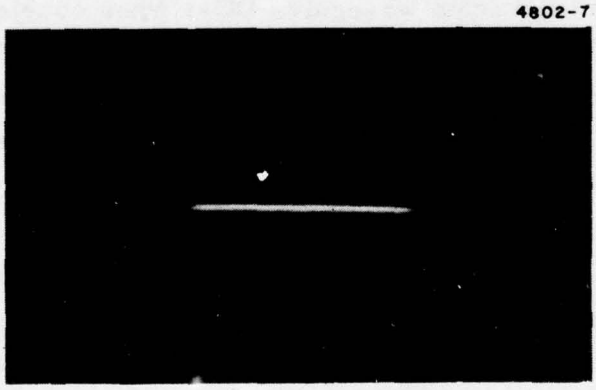

Figure 15. Near field photograph of waveguide light.

S = 5 modes. The m-lines were clearly visible when viewed with a "snooperscope" on a ground glass screen placed several centimeters from the prism, and the relative power in each mode could be measured with the calibrated Si photodiode. The coupling efficiency of the prism was between about 10 to 40% and varied depending on clamping pressure and quality of surface contact. Thus only the relative power in each mode could be measured rather than the absolute power. The power in each mode and the coupling efficiency into each mode were then determined by assuming that the total power transmitted by the waveguide (as measured with the calibrated Si detector) was divided between the various modes in the same proportions as the relative powers measured in the m-lines. The validity of this assumption was supported by the fact that the relative proportions of power in each mode remained constant when the prism was moved to various positions along the waveguide and was always repeatable even though the absolute power levels measured varied considerably, depending on prism clamping pressure, etc. The constancy of these ratios also indicates that inter-mode coupling or mode conversion was not occurring as the light traveled along the waveguide. Since all of the modes observed in these waveguides were well confined and far from cutoff we also assumed that the prism coupling efficiency was the same for all modes. Any error introduced by this assumption would tend to make the resulting calculated power in the lowest order mode appear less than actual and the values for higher order modes appear greater than actual. This is because the lowest order mode is theoretically better confined than the higher order ones (which are closer to cutoff) and therefore the prism coupling efficiency should be worst for the lowest order mode. Thus the values for power coupled into the lowest order mode that we have determined are conservative.

In the course of perfecting our alignment techniques, a great many measurements of total power coupled and modal distribution were made. However the significant data can be concisely summarized as shown in Table 4 where only the best results achieved for each waveguide are tabulated, since these represent the closest we were able to

come to ideal alignment in each case. It should be noted that the efficiencies shown in Table 4 are actually overall transmission efficiencies rather than input coupling efficiencies since they have not been corrected for either waveguide attenuation or for reflection loss at the output of the waveguide.

Looking at these raw data one can see the significant effect of waveguide attenuation in that the efficiencies for long waveguides are much less than those for short ones. From the dependence of measured efficiency on waveguide length, we estimate the waveguide attenuation to be approximately 2 dB/cm. In the case of waveguide DC-2 detailed measurements were made of the attenuation loss. A laser diode was coupled to the waveguide and clamped in position to maintain constant input coupling. Then the output coupling prism was moved to various positions along the length of the waveguide and the relative power in each mode was measured as previously described. There was a significant scatter in the data, probably because of variations in the prism coupling efficiency from one spot to another. Nevertheless we were able to determine loss coefficients by drawing a straight line through the points on a semilog plot of relative power versus distance. The results indicated the following losses for the three modes observed:

S = 1	1.6 dB/cm
S = 3	1.6 dB/cm
S = 5	1.8 dB/cm

The reflection loss at a Ta_2O_5 waveguide output to air is

$$R = \left(\frac{n_2 - n_1}{n_2 + n_1}\right)^2 = \left(\frac{2.0-1}{2.0+1}\right)^2 = 0.11$$

When the measured efficiency data of Table 4 for Ta_2O_5 waveguides are corrected for the above output reflection losses, and also for an assumed waveguide attenuation of 1.6 dB/cm for waveguide DC-2 and 2 dB/cm for the others the values shown in Table 5 result. These values probably more accurately represent the actual input coupling

TABLE 4. MEASURED COUPLING EFFICIENCIES BASED ON TRANSMITTED POWER UNCORRECTED FOR WAVEGUIDE LOSSES

4716-2 R1

LABEL	WAVEGUIDE			LASER EMITTED POWER W	WAVEGUIDE TRANSMITTED POWER W	EFFICIENCY (PERCENT OF LASER EMITTED POWER)			
LASER WAVEGUIDE	MATERIAL	THICKNESS μm	LENGTH cm			TOTAL	MODE S = 1	MODE S = 3	MODE S = 5
LD67-8 DC-2	Ta_2O_5	1.0	4.0	12.8	0.65	5.0	4.0	0.81	0.19
LD69-1 RF-1	Ta_2O_5	1.7	4.0	16	0.84	5.2	4.4	0.8	—
LD67-3 DC-1	Ta_2O_5	2.0	4.0	16	1.04	6.5	5.2	1.3	—
*LD67-7 DC-1	Ta_2O_5	2.0	1.9	12.8	2.39	19	17.0	2.0	—
LD69-2 RF-1	Ta_2O_5	1.7	0.7	2.08	0.56	27			
LD69-1 DC-1	Ta_2O_5	2.0	0.7	16	8.32	52			
*LD67-9 R-1	7059 GLASS	1.0	4.5	23.9	3.06	12.8	11.3	1.5	—

*HYBRID DELIVERED TO AIR FORCE

TABLE 5. COUPLING EFFICIENCIES CORRECTED FOR WAVEGUIDE ATTENUATION AND OUTPUT REFLECTION LOSS

CORRECTED FOR WAVEGUIDE LOSS

4716-2 R2

LABEL	WAVEGUIDE			LASER EMITTED POWER W	COUPLED WAVEGUIDE POWER W	COUPLING EFFICIENCY (PERCENT OF LASER EMITTED POWER)			
LASER WAVEGUIDE	MATERIAL	THICKNESS μm	LENGTH cm			TOTAL	MODE S = 1	MODE S = 3	MODE S = 5
LD67-8 DC-2	Ta_2O_5	1.0	4.0	12.8	3.19	24.9	20.0	4.0	0.9
LD69-1 RF-1	Ta_2O_5	1.7	4.0	16	5.94	37.1	31.3	5.8	—
LD67-3 DC-1	Ta_2O_5	2.0	4.0	16	7.36	46.1	36.9	9.2	—
*LD67-7 DC-1	Ta_2O_5	2.0	1.9	12.8	6.44	50.3	45.1	5.2	—
LD69-2 RF-1	Ta_2O_5	1.7	0.7	2.08	0.87	41.6			
LD69-1 DC-1	Ta_2O_5	2.0	0.7	16	12.9	80.6			

*HYBRID DELIVERED TO AIR FORCE

efficiencies achieved than do the uncorrected data of Table 4. However, even if one takes the more conservative viewpoint and does not correct for waveguide attenuation and output reflection loss it is obvious that the program goal of 1 W coupled into the lowest order mode was significantly exceeded in the two laser/waveguide hybrids that were delivered (LD67-7/DC-1 and LD67-9/R-1).

Before concluding this section on butt coupling power and efficiency we should mention that the angle-butt coupling arrangement shown in Fig. 2 was also experimentally tested, even though the theory predicted that coupling efficiency would be lower than that for the collinear butt coupling case. Samples of waveguides DC-1 and RF-1 0.7 cm in length were polished on one end to an angle of 55^{o} while the other end of each sample was polished at the usual 90^{o} angle to permit measurement of emitted power. Laser diode LD-69-1 was butt coupled to each of these samples by means of a special fixture which held it at 55^{o} to the direction of propagation in the waveguide. The best transmission efficiencies we were able to achieve were 21% for waveguide RF-1 and 35% for waveguide DC-2. Comparing these with the corresponding values of 27% and 52% obtained with collinear butt coupling to 0.7 cm long samples of RF-1 and DC-1 (see Table 4) supports the theoretical prediction of lower efficiency for angle butt coupling.

B. Rockwell Waveguide/Lens Samples

Three of the waveguides supplied by the Air Force (listed in Table 2 as R-1, R-2, and R-3) were sputtered 7059 glass waveguides with overlayed Ta_2O_5 lenses. These were fabricated by Rockwell International under separate contract with the Air Force Avionics Laboratories. The coupled power and efficiency data for the LD67-9/R-1 hybrid have already been discussed in Section IV-A. In this section we comment specifically on the performance of the lenses, which were designed to collimate the diverging beam of coupled light after it had spread to a width of approximately 1 cm.

The LD67-9 laser diode emitting a peak power of 23.9 W was coupled to R-1, a waveguide with a double convex shaped Ta_2O_5 lens. The lens is visible in Fig. 16, which shows the operating hybrid. No polishing of the waveguide was done prior to coupling because fortunately there was a clean straight-broken edge at exactly the right position for aligning the laser with the lens (which was offset from the center of the waveguide). Visual observation of the transversely scattered light with a snooperscope revealed an apparent collimation of the waveguided laser beam by the lens, from a full-width half-maximum (FWHM) divergence angle of approximately 30° to one of less than 10°. This collimation is shown in Fig. 17 which is an infrared photograph of the coupled laser beam. Because the response of the film to the scattered light from the beam is not linear the details of the beam shape are difficult to see. However, after being coupled in at the left hand edge the beam diverges until it reaches the lens, located about 2/3 of the way along the waveguide. After passing the lens the beam appears as a collimated band, with a width slightly less than that of the lens. The alternating bright and dark bands visible after the light passes the lens seem to be due to interference between the waveguided beam and unguided light reflecting from the back surface of the substrate where it is pressed against the copper waveguide holder. These interference lines are not visible at the far right end of the photograph where the waveguide sample protrudes out of the holder by about 0.5 inch and is backed with a piece of black tape. It is in this region that the collimated beam can be seen most clearly. The random bright spots are caused by specks of dust which unavoidably settled on the waveguide during the 20 minute time exposure required to make the photograph. (The film used was Kodak Ektachrome Infrared.)

When an output coupling prism was put on the waveguide two m-lines were observed. As viewed with the snooperscope on a translucent screen spaced 10 cm from the prism, the two modes appeared to have full width half maximum divergence angles of 9° for the lowest order mode and 6° for the higher order mode. By comparison the corresponding divergence angle for the LD67-8 laser and DC-2 Ta_2O_5

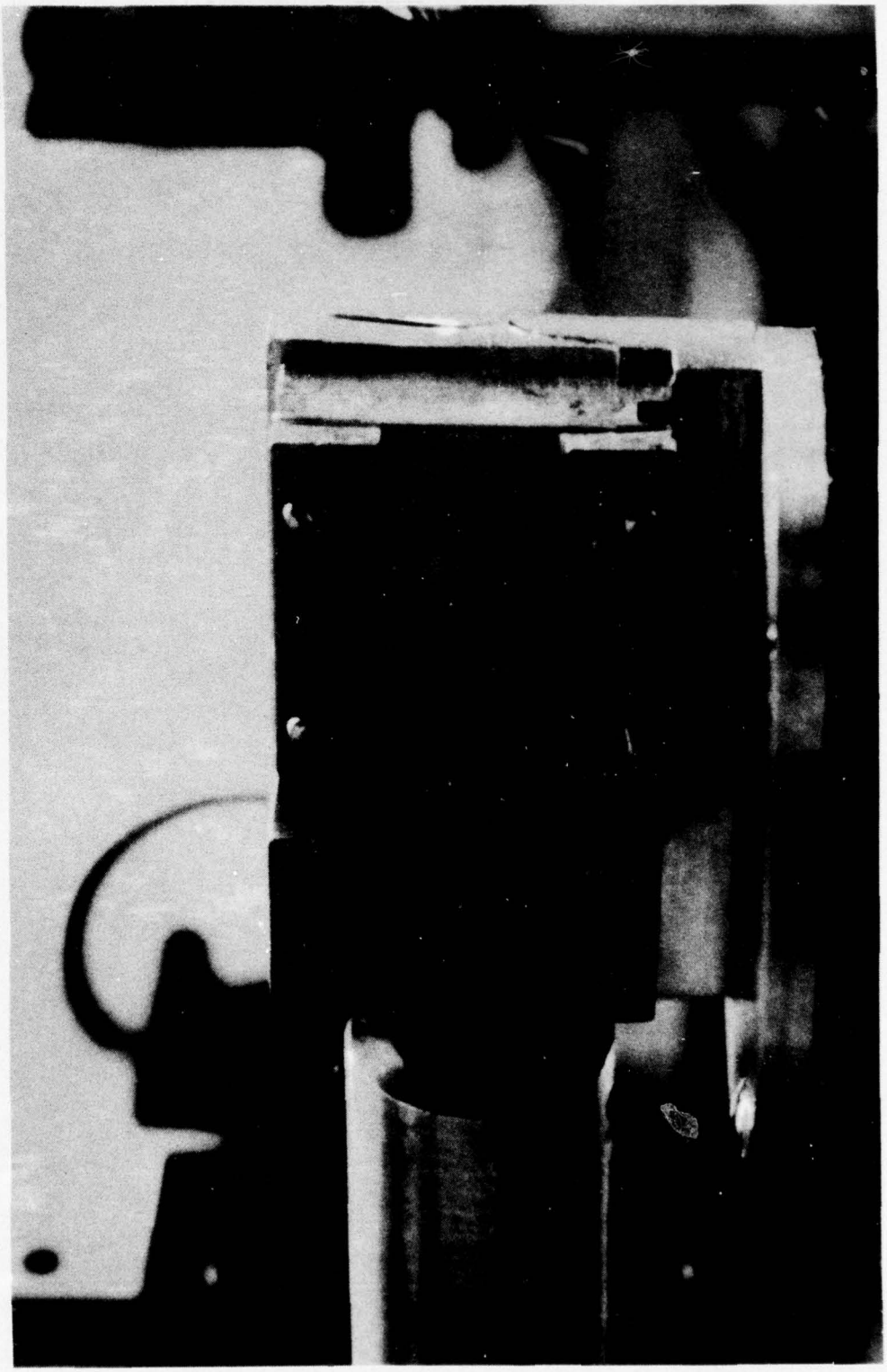

Figure 16. Operating laser/waveguide hybrid (with collimating lens).

M11731

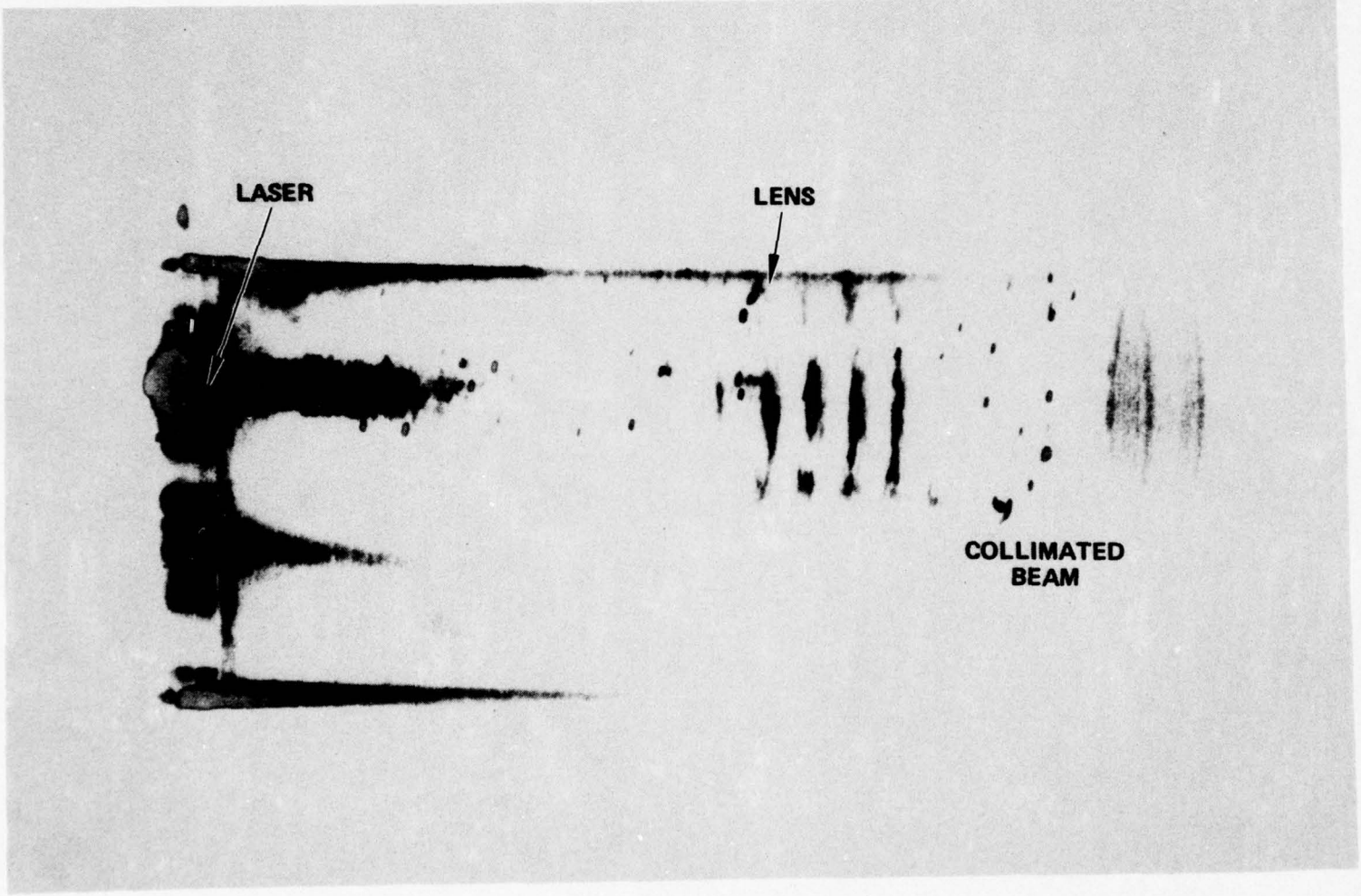

Figure 17. Infrared photograph of coupled laser beam in 7059 glass waveguide with Ta_2O_5 collimating lens.

waveguide hybrid was measured in the same way to be approximately 20° for all three m-lines. To obtain quantitative data the two m-lines of the LD67-9/R-1 hybrid were scanned with the Si detector, masked to a 1 mm square aperture. The results indicated FWHM divergence angles of 8° for both modes. Thus the apparent narrower divergence of the higher order mode as observed visually seems to merely be the result of the low power level in that mode and the nonlinear response of the eye.

We attempted to couple light into waveguide R-2 with the round spot shaped lens (see Table 2) but the scribed and broken edge was too rough to permit significant coupling. Unfortunately when we tried to polish the waveguide using our standard technique described in Section III it cracked, destroying the lens and preventing further experiments with it.

C. Coupling of cw Laser Diodes

The LCW-5 laser diode described in Section III was butt coupled to waveguide R-3. Prior to coupling the waveguide sample was polished on both ends so that close coupling would be possible and that transmitted optical power could be measured. In coupling the cw laser to a waveguide there are two competing factors affecting the coupling efficiency as compared to that obtainable with a pulsed laser of the type we have used. The nominal emitting layer thickness of the cw laser is only 0.25 μm compared to 2.0 μm for the pulsed laser. This is expected to produce better coupling efficiency by minimizing area mismatch. However, because of diffraction the cw laser has a FWHM divergence angle of 50° in the plane perpendicular to the junction rather than 10° as is the case for the pulsed laser. Therefore, the spacing between the cw laser and waveguide is much more critical than that for the case of the pulsed laser. This proved to be the limiting factor for the particular LCW-5 laser that we used. Although the laser diode appeared to be flush with the edge of the heatsink as required for close coupling, we found that it was actually set back about 0.001 in. The heatsink edge was rounded, giving the appearance of flush mounting.

Because of this setback true close coupling could not be achieved. Nevertheless a cw power of greater than 0.74 mW was coupled into the waveguide as determined by transmitted power measurements. Since the laser emitted power for a current of 310 ma was 7.5 mW, this corresponded to a transmission efficiency of approximately 10%. The actual coupling efficiency was of course greater than 10% as that value is uncorrected for waveguide loss. In order to achieve greater coupling efficiency with a cw laser it will be necessary to have one in which the laser diode is carefully positioned for flush mounting on a specially machined heatsink with a square edge. Since especially good heatsinking is required for cw operation it will not be sufficient to merely mount the laser diode so that it is protruding over the edge of a standard production heatsink.

SECTION V

COMPARISON OF THE RESULTS ACHIEVED WITH THEORETICAL PREDICTIONS

A. Coupling Efficiency

In Section II a theoretical expression was derived for the coupling coefficient $|A_s|^2$ for the case of parallel end butt coupling (Eq. 15). Figure 18 shows the normalized curves of $|A_s|^2$ versus the ratio of waveguide thickness (t_g) to laser light emitting layer thickness (T_L). The solid curves are the theoretical curves for the three lowest order TE modes in the case of $t_L = 2.0$ μm, the nominal emitting layer thickness for the LD-69 and LD-67 type lasers. The plotted points are the experimentally measured values of coupling coefficients (efficiencies) from Table 5. It will be recalled that these values have been corrected for waveguide loss and output reflection loss as described in Section IV. Thus they represent the best estimate of true input coupling efficiencies. It can be seen from Fig. 18 that the experimentally determined data for the S = 1 mode fall significantly below the theoretical curve, while the data points for the higher order modes are above the theroetically expected values. This is particularly evident for the case of the 2.0 μm thick waveguides where $t_g/t_L = 1$. One possible explanation for this discrepancy is that we have just not achieved the perfect alignment for which the theory is derived. However we feel that the actual reason for the difference between theory and experiment is that the 2.0 μm light emitting layer thickness specified by the laser manufacturers is not the true thickness of the emitting layer. The scanning electron microscope measurements described in Section III clearly show that the distance between the p-n junction and the GaAs-(GaAl)As heterojunction is indeed 2.0 μm (see Fig. 3). However light which is generated in this 2.0 μm thick active (or inverted population) region of the laser tends to spread out of it because of diffraction. On one side of the junction the light is confined by reflection

at the GaAs-(GaAl)As heterojunction but on the other side it is able to spread, thus increasing the thickness of the light emitting layer. The optical measurements of the near field pattern of an LD-69 laser that were described in Section III in fact indicated that the emitted light had an essentially Gaussian mode shape in the direction normal to the junction plane with a FWHM thickness of approximately 5 μm. The fact that the light emitting layer thickness is ≃5 μm reduces the achievable coupling efficiencies below those predicted by theory based on the assumption of t_L = 2 μm as in Fig. 18. If the same experimental data points are plotted as shown in Fig. 19, assuming a laser light emitting layer thickness of 5.8 μm the agreement with the theoretical curves is much better. The specific choice of t_L = 5.8 μm rather than just t_L ≃5 μm is based on a fitting of the experimental data to a theoretical curve giving the variation of coupling efficiency with lateral transverse misalignment of the laser and waveguide. These tolerance data are described in the next paragraph.

B. Tolerances

The tolerance to transverse displacement of the laser relative to the waveguide was experimentally studied by butt coupling laser LD-67-8 to waveguide DC-2 with the alignment fixtures, then intentionally moving the laser laterally in the transverse (x) direction by changing the voltage on the piexoelectric micrometer. Because of the high resolution of the PZM micrometer (40 A/V) an accurate curve of relative coupled power versus laser displacement was obtainable. The results are shown in Fig. 20. The solid curves are the experimentally measured coupled power data for the three lowest order modes, while the dotted curve is the theoretically expected coupled power variation for the fundamental mode assuming a laser light emitting layer thickness T_L = 5.8 μm. This value of thickness was chosen to fit the experimental data to the theoretical curve for laser displacements toward the surface (+x) of the waveguide. The broadening of the experimental

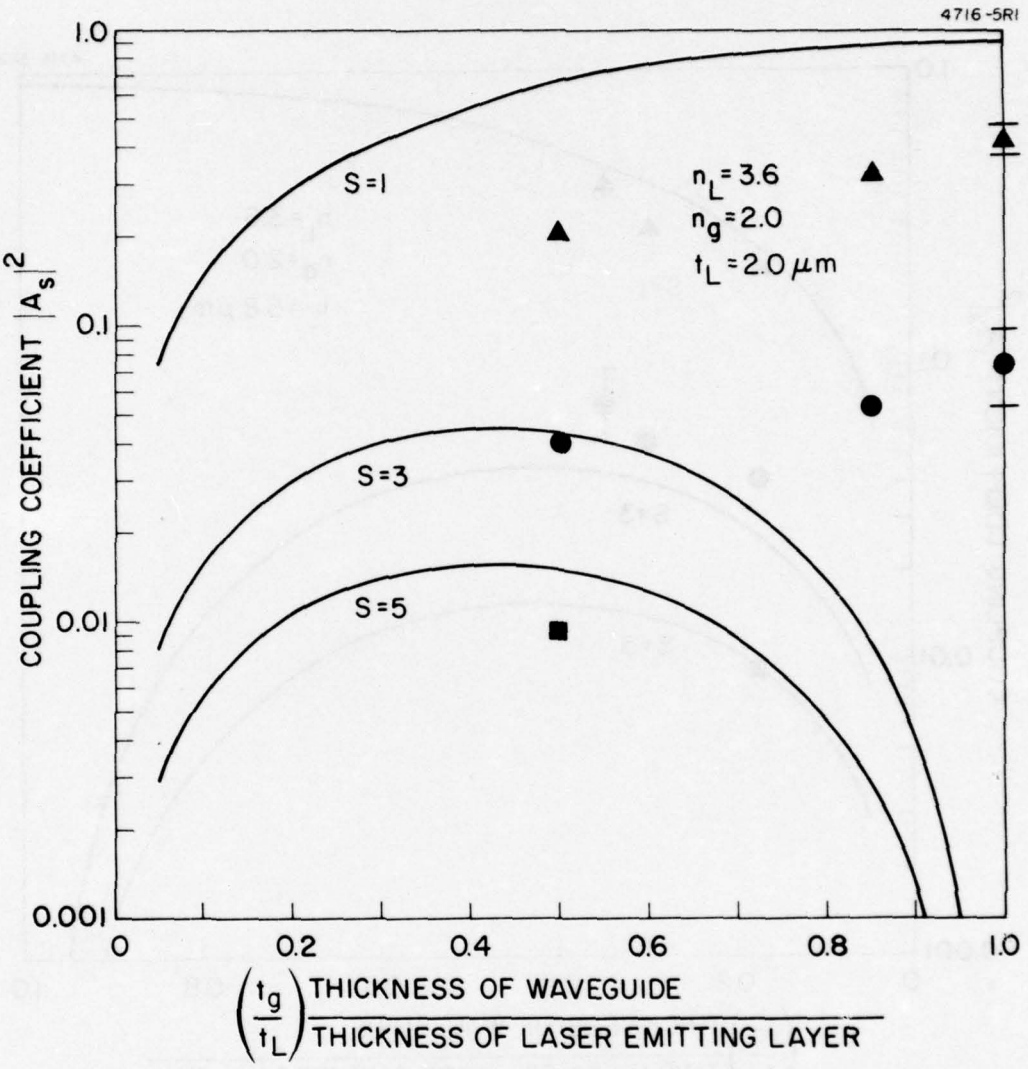

Figure 18. Comparison of theoretical and experimental coupling coefficient data for t_L = 2.0 μm.

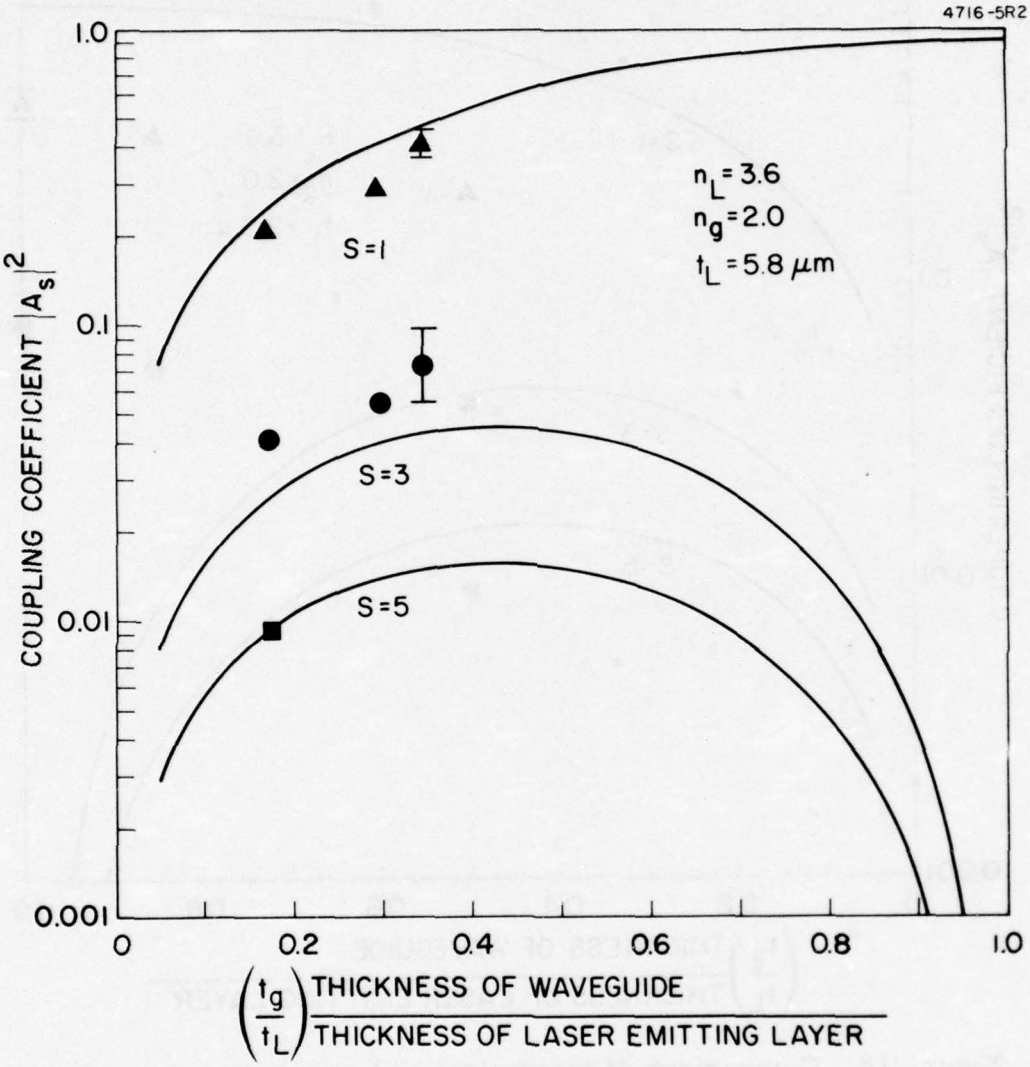

Figure 19. Comparison of theoretical and experimental coupling coefficient data for $T_L = 5.8\ \mu m$.

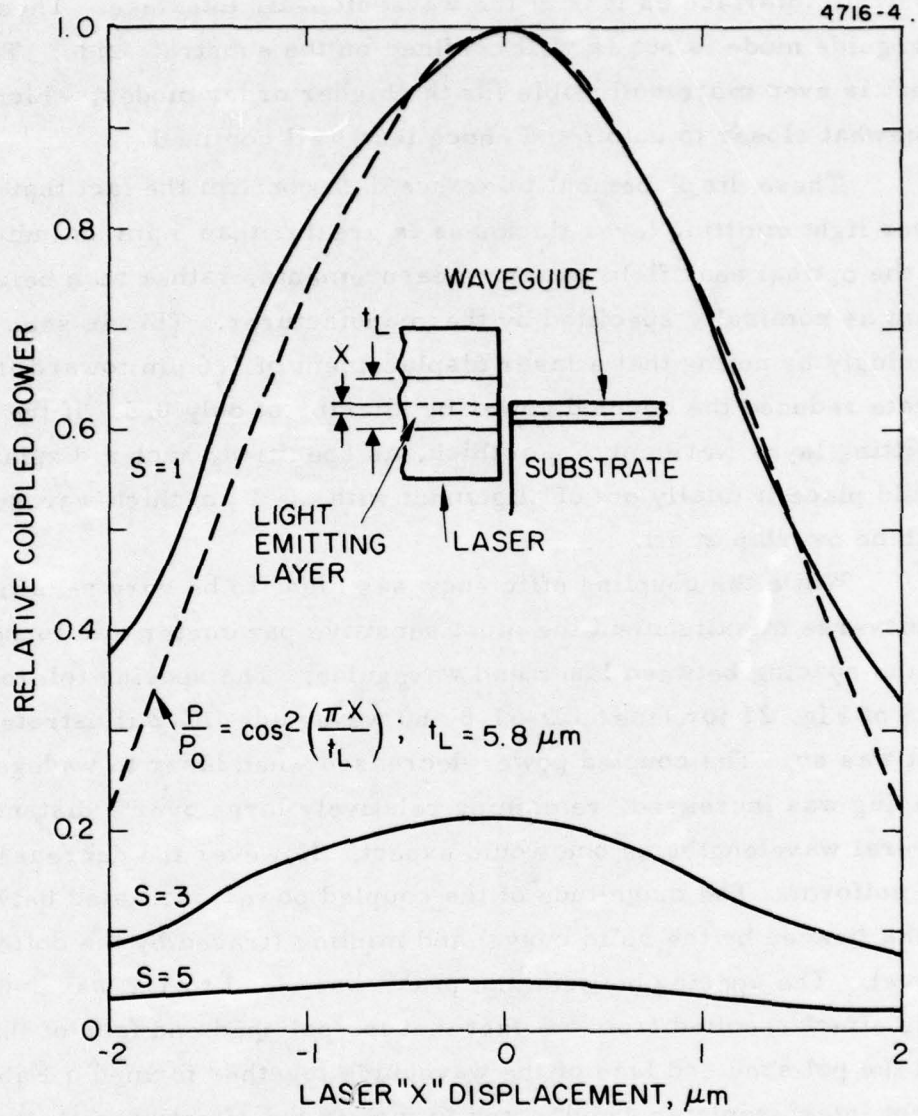

Figure 20. Tolerance to transverse displacement.

curve for laser displacements toward the substrate (-x) results because the step in the index of refraction profile is not as great at the waveguide-substrate interface as it is at the waveguide-air interface. Thus the waveguide mode is not as well confined on the substrate side. This effect is even more noticeable for the higher order modes, which are somewhat closer to cutoff and hence less well confined.

These displacement tolerance data confirm the fact that the laser light emitting layer thickness is greater than 5 μm as indicated by the optical near field pattern measurements, rather than being just 2 μm as nominally specified by the manufacturer. This is seen convincingly by noting that a laser displacement of 1.6 μm toward the substrate reduced the coupled power by a factor of only 0.5. If the laser emitting layer were only 2 μm thick, as specified, such a displacement would place it totally out of alignment with the 1 μm thick waveguide, with no overlap at all.

While the coupling efficiency was found to be very sensitive to transverse misalignment the most sensitive parameter was found to be the spacing between laser and waveguide. The spacing tolerance data of Fig. 21 for laser LD-67-8 and waveguide DC-2 illustrate why that was so. The coupled power decreased when laser to waveguide spacing was increased, remaining relatively large over a distance of several wavelengths as one would expect. However the decrease was not uniform. The magnitude of the coupled power oscillated between peaks (traced by the solid curve) and minima (traced by the dotted curve). The spacing between the peaks was equal to 1/2 wavelength. This effect resulted from the fact that the polished end face of the laser and the polished end face of the waveguide together formed a Fabry-Perot interferometer which acted to modify the effective reflectance of the laser output face, thereby altering the coupled power. The practical significance of this observation is that the resolution of the adjustment to laser-waveguide spacing must be better than 0.1 μm to enable one to obtain peak coupling efficiency, even though the total spacing can be as much as 4 μm without causing more than a factor of 0.5 decrease in coupled power. The Fabry-Perot interferometer effect

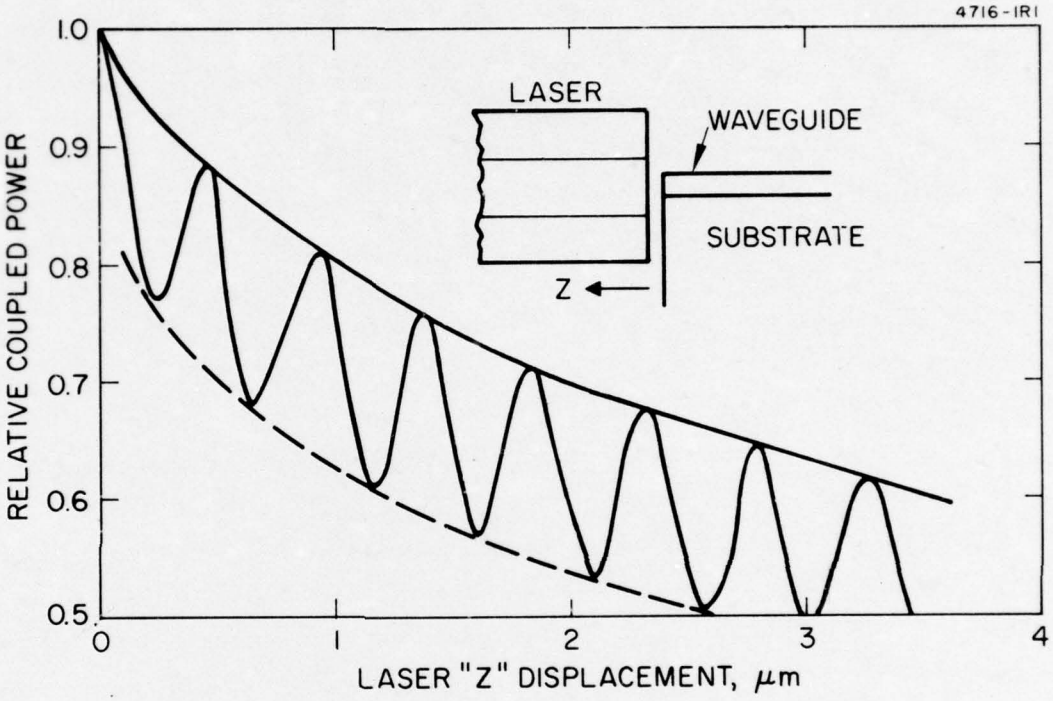

Figure 21. Tolerance to laser/waveguide spacing.

could in principle be eliminated by using an index matching fluid or epoxy between the laser and waveguide. However the practical difficulties in achieving a stable match appear to be prohibitive for the limited improvement in coupling that would result.

SECTION VI

CONCLUSIONS AND RECOMMENDATIONS

The work described in this report has established that the parallel end butt coupling method is a viable technique for coupling an injection laser to a thin film waveguide. Theoretical calculations predict that most of the optical power is coupled into the lowest order mode, and that coupling efficiencies into that mode as high as 90% can be achieved for the case of a GaAs laser and Ta_2O_5 waveguide both with the same thickness light emitting or guiding layer. As the thickness of the waveguide is decreased relative to that of the laser the coupling efficiency into the lowest order mode is decreased and more power is coupled into the higher order modes. However, even for a ratio of $t_g/t_L = 0.5$ the theoretical maximum coupling into the lowest order mode is 60% while that into the next higher (S = 3) mode is 4%. The theory also predicts that angling the end face of the waveguide to increase effective area does not improve the coupling efficiency because the competing reduction in coupling resulting from misalignment of the optical fields in the laser and waveguide is dominant. Thus the parallel end butt coupling collinear with the waveguide is best. The experimental results achieved agree well with the theoretical predictions. Overall transmission efficiencies determined by measuring power emitted from the waveguide were as high as 52% for the case of a 2.0 μm thick waveguide. When this value was corrected for waveguide attenuation and output reflection loss the calculated input coupling efficiency was 80%. Measurements of modal power distribution confirmed that more than 80% of the power coupled into the waveguide went into the lowest order mode in all of the cases examined. Only the S = 1, 3, and in some cases S = 5 modes were observable in the waveguides, as predicted by the theory.

The two laser/waveguide hybrids that were delivered had lowest mode coupled powers of at least 2.39 W and 3.06 W corresponding to coupling efficiencies of 17% and 11.3%, respectively. These are very

conservative values because they are based on measurements of power emitted from the waveguide, uncorrected for waveguide attenuation and output reflection loss. Nevertheless, they exceed the program goal of 1 W coupled into the lowest mode with 10% efficiency. If the waveguide loss corrections are made as described in Section IV, the calculated values of coupled power into the lowest mode and coupling efficiency become 6.44 W and 45.1% for the LD-67-7/DC-1 (Ta_2O_5) hybrid. We feel that these are probably more realistic values than the 2.39 W and 17% uncorrected ones.

One important fact that emerged from the coupling experiments was that the thickness of the light emitting layer in the single heterojunction lasers that were used was greater than 5 μm, even though the light generating layer was 2 μm as specified by the manufacturer. This thicker light emitting region must be taken into consideration when calculating the theoretical coupling efficiency in any given case, since efficiency is reduced for smaller values of t_g/t_L.

In order to achieve the coupling efficiencies that have been reported, critical alignment of the laser and waveguide necessitates the use of piezoelectrically driven fixtures or some equivalent means. The spacing between the laser and waveguide and the transverse lateral waveguide-laser alignment are the most critical parameters, requiring an adjustment resolution of better than 0.1 μm to ensure optimum coupling. Piezoelectric micrometers with resolution of 40 Å/V were effective in this application. The various tilt and rotational alignment parameters were found to be much less critical, and could be adjusted for optimum coupling with a relatively unsophisticated mechanical stage.

Laser diodes had to be specially ordered mounted flush with the edge of the heatsinks and without caps and windows to permit close coupling with the waveguides. However these slightly modified versions of the basic production laser diode were available at only a small price increase over that of the standard diodes. Because the laser diodes were flush with the edge of the heatsink, or in some cases protruding slightly, extreme care had to be taken during alignment to prevent chipping either the laser or the waveguide by butting them together.

For this reason final alignment was always performed with only the piezoelectric adjustments. Once optimum alignment was achieved the laser and waveguide were bonded together by means of the eight clamping setscrews on the waveguide support structure. Tightening of these setscrews as a delicate task to avoid destroying the alignment in the process. However we found that it was possible to tighten the setscrews to the point where the Allen wrench would begin to bend while still maintaining optimum alignment, as long as one was careful to adjust opposing setscrews alternately while monitoring the coupled power with the Si detector. Once clamped in this fashion the laser/waveguides could be removed from the alignment fixtures and handled with normal care without any shift in alignment.

Ultimately it should be possible to obtain even better coupling efficiency with a cw laser than with the pulsed laser diodes which we used. This is true because the cw lasers are double heterojunction diodes with light confinement on both sides of the p-n junction to an emitting layer thickness of 0.25 μm. Compared to the 5 μm emitting layer thickness of pulsed diode lasers this offers a potential advantage of a factor of 20 in increased t_g/t_L ratio. However increased beam divergence due to diffraction in the cw laser makes close spacing of the laser and waveguide absolutely imperative. The need for the laser to be flush mounted or protruding on the heatsink presents a particular problem in the case of present day cw lasers which require extremely good heatsinking. As improvements in laser and heatsink design are made this problem will become less significant.

REFERENCES

1. M. C. Hamilton and D. A. Wille, "Acousto-Optic Diffraction in Optical Waveguides," Technical Digest of the Optical Society of America Topical Meeting on Integrated Optics, Jan. 21-24, 1974, New Orleans, LA

2. R. G. Hunsperger and A. Lee, "Parallel End-Butt Coupling of a GaAs Laser Diode and a Thin Film Waveguide," Technical Digest of the Optical Society of America Topical Meeting on Integrated Optics, Jan. 12-14, 1976, Salt Lake City, Utah.

3. Amnon Yariv, "Coupled Mode Theory for Guided-Wave Optics," IEEE Journal of Quantum Electronics QE-9, 919 (1973)

ACCESS COUPLING OF A SINGLE OPTICAL FIBER

INTRODUCTION

Recent advances in the field of fiber optics have made feasible the use of single fibers as a communication channel. In order for a single fiber to service a system of many terminals, it is necessary to develop a low insertion loss optical access coupler. The purpose of this portion of the contract was to further the state of the art in this area.

Among the different methods for coupling between single fibers are coupling by close proximity of air coupled fiber cores, coupling by adding an index matching medium between the fibers, and coupling by fusing the cladding of the two fibers together. This effort was conducted using the clad fusing technique. The source of heat was a 2 W CO_2 laser and the fibers were Corning low loss, step index, multimode fibers with an 85 μm core diameter and a 125 μm outside diameter.

WELDING TECHNIQUES

The technique by which the fibers are held has a great effect on the results of the fusing process. Three different holding fixtures, circular, straight and curved, were used. The circular holding fixture which is shown schematically in Fig. 1 was used initially. Originally the fibers were loaded directly into shallow grooves on the 2-1/2 in. diameter aluminum cylinders. This proved to be too great a heat sink for the laser power density available at that time (beam power = 2 W, lens = 6 in. focal length). Hence, ceramic inserts were added

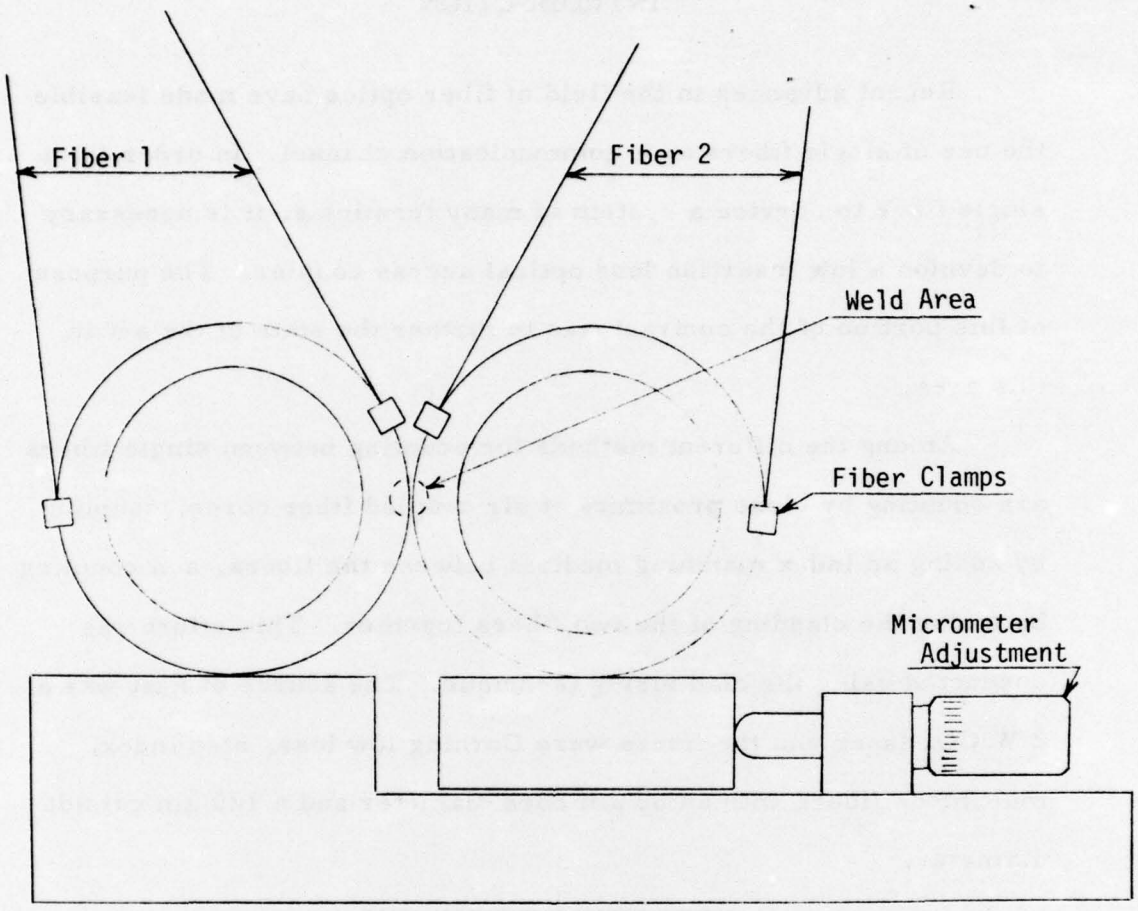

Fig. 1. Circular Holding Fixture.

behind the fibers in the area of the weld, but this had little effect on the excessive heat sinking. A small flat area was then ground behind the fibers in the area of the weld. This removed the heat sink and allowed sufficient heating of the fibers for fusion to take place. Since the fibers were not restrained both in front and back (in the plane of bend), they tended to move in an uncontrolled manner as tensions were relieved during the heating process. This made repeatable fusion almost impossible and was sufficient reason to develop a new type holding fixture.

In an attempt to eliminate the uncontrolled motion of the fibers as they were heated, a fixture was designed to hold the two fibers in contact with each other and in a straight and unstressed manner. This straight holding fixture (Fig. 2) solved the motion problem as long as care was taken in placing the fibers in the fixture and they were free of static charge. The length of the weld was determined by translating the fixture relative to the laser beam so that the beam "scanned" the junction of the two fibers. It proved too difficult to obtain a smooth weld over any reasonable distance with the small focused spot of the spherical lens. A one-inch focal length cylindrical lens was purchased to replace the spherical lens. The combination of the new lens and this fixture (Fig. 2) has been very successful and has provided all the best results obtained to date. Welds as long as 1.3 cm can be made at one time. One 3 cm long weld was made by welding, moving the fiber pair on the fixture and then continuing the weld.

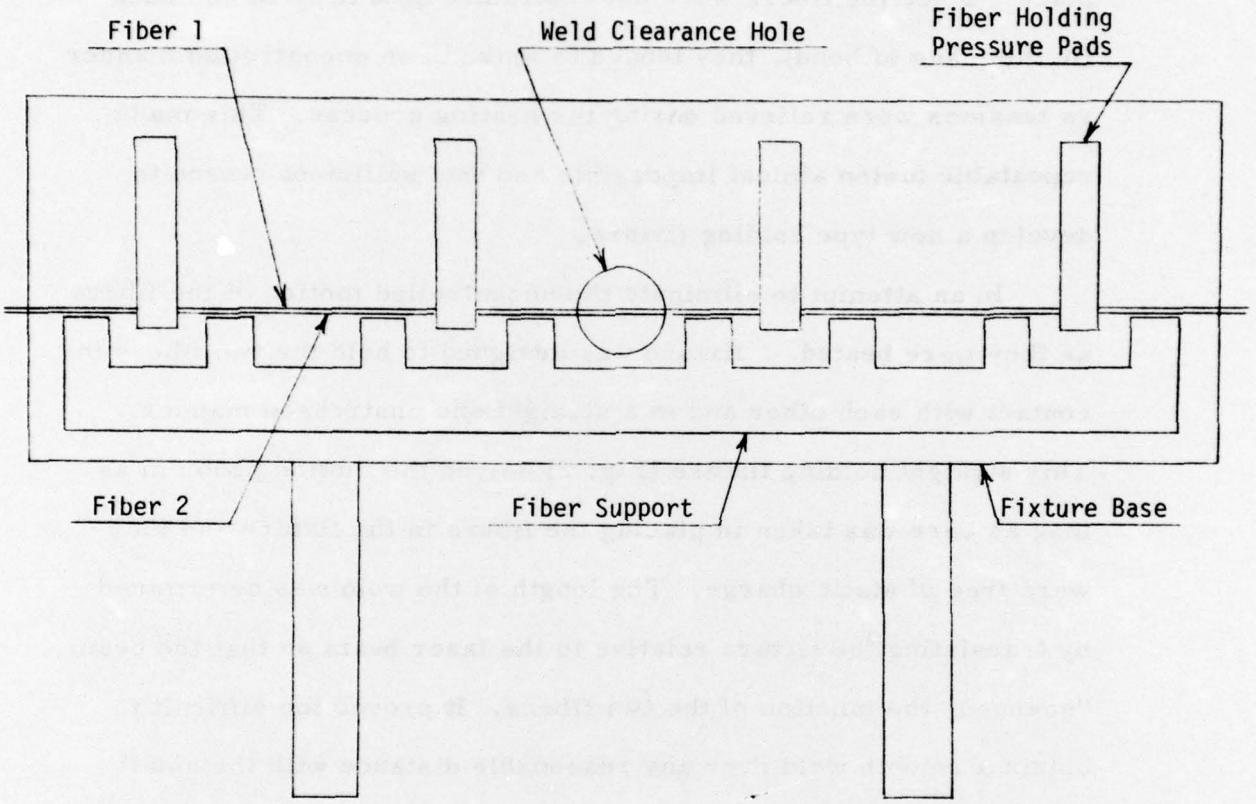

Fig. 2. Straight Holding Fixture.

It was felt that better coupling might be obtained over a shorter distance if the fibers could be welded while radiused rather than straight. The results of the circular holding fixture indicate that the fibers must be supported along their entire length in the fixture if they are to remain still while being heated. This in turn requires higher power density to offset the fibers being heat sunk to the fixture. In order to obtain a higher power density, a short focal length (1.5 inches) spherical lens was obtained. Figure 3 shows this curved holding fixture. The radius of curvature of the fiber holding pieces is 25 cm. Although the power density was sufficient to make the weld, the spherical lens again produced an uneven weld and indicated the need for the cylindrical lens. This time the combination of the one inch focal length cylindrical lens and the 2 W laser did not produce sufficient power density to make a weld. An attempt is being made to secure a higher power CO_2 laser.

MEASUREMENTS

Tap ratio and insertion loss measurements were made on the couplers. The tap ratio and insertion loss are defined as

$$\% \text{ Tap} = \frac{P_4}{P_1} (100)$$

$$\text{Insertion Loss} = 10 \log \frac{P_4 + P_3}{P_1}$$

where P_1 is the power into the original fiber, P_3 is the power out of the original fiber after tap and P_4 is the power out of the tap fiber.

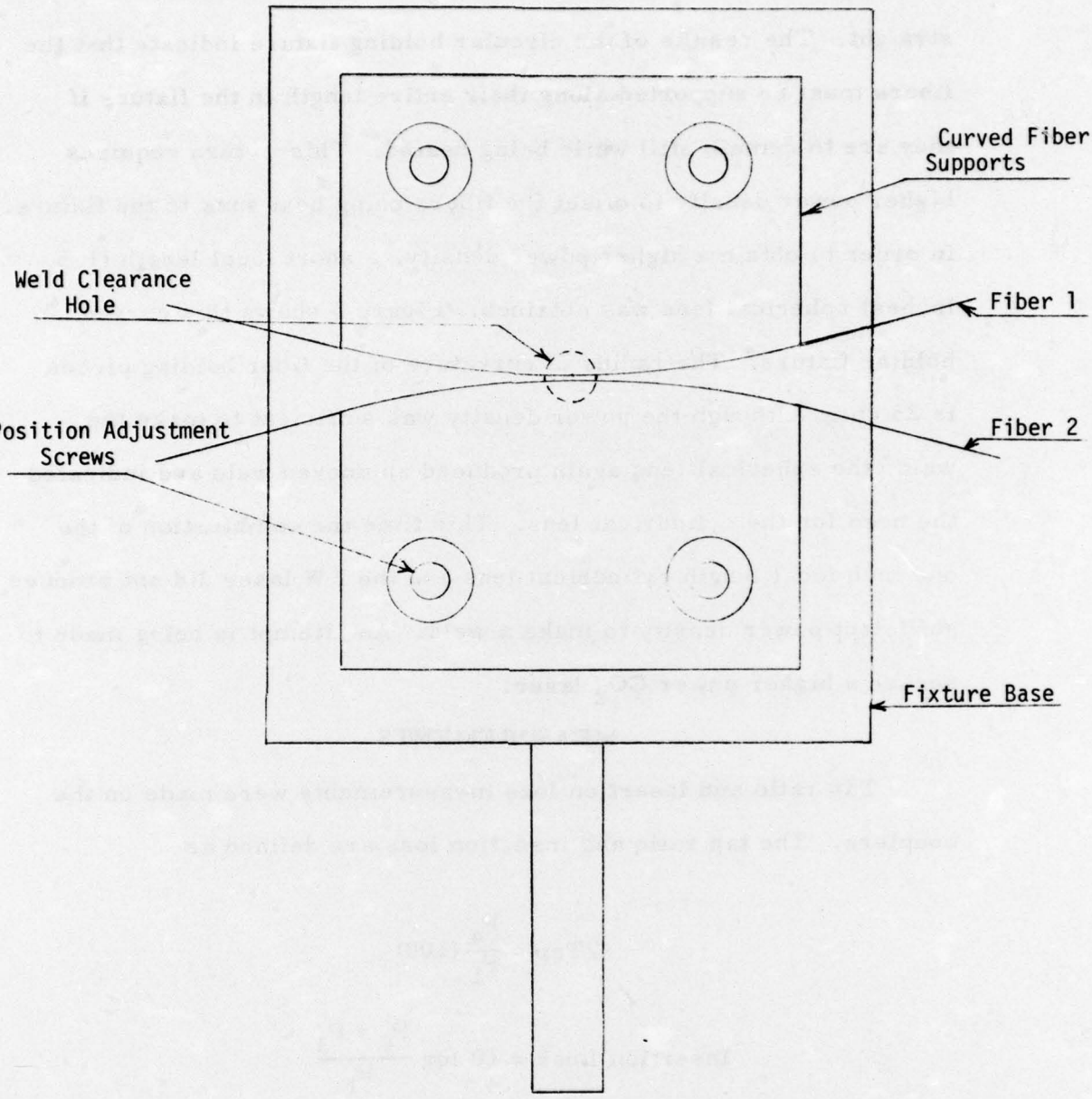

Fig. 3. Curved Holding Fixture.

The measurement of the tap ratio data is straight forward. The output powers P_3 and P_4 were measured, usually with a United Detector Technology Model 80X or Model 111A detector, after the coupling weld was made. However, the insertion loss measurements were somewhat more complicated. Because of the particular arrangement in the laboratory, it would have been more convenient to be able to measure P_1, remove the input fiber from the test source, go to the CO_2 laser and make the coupler, return to the test source with the input fiber and measure P_3 and P_4. No satisfactory fixturing was found to ensure that P_1 was the same before and after the tap. Hence, the following two methods were employed instead: (1) the input fiber was left in its holder while making the weld, or (2) the weld was made, P_3 and P_4 were measured and then the input fiber was cleaved with the source in place and P_1 measured.

All of the measurements were made with a glycerol saturated felt pad mode stripper on the input fiber, a short distance from the source. During the initial phase of this work the tap data was taken with the coupler itself held in a large mode stripper. This was found to result in a higher measured insertion loss than that obtained if the junction region were left suspended in free space and the cladding mode stripping accomplished separately at each port of the access coupler. This could be attributed to the excitation of cladding modes in the junction region which couple back to core modes when leaving the junction region if they have not already been stripped away with an external mode stripper.

RESULTS

A total of 21 access coupler (numbers 11 through 32) were made during this portion of the contract. Results of earlier couplers were typically not repeatable and had a very low tap ratio with low insertion loss or a higher tap with high insertion loss. The later couplers showed much improvement in repeatability, tap percentage and insertion loss as shown in the following table.

Coupler No.	Insertion Loss (dB)	% Tap
18	-0.08	0.17
19	-5.02	3.9
29	-2.9	7.9
30	-1.0	2.9
31	-1.9	6.2
32	-1.1	6.6

The devices delivered were couplers 29 to 32.

A photograph of the output of a coupler is shown in Fig. 4 along with a schematic drawing of a coupler. Figure 5 is a photograph of coupler number 32 with a blow-up of one end at the welded section. The photograph in Fig. 6 shows a cleaved end of a welded junction. Note that the cores show little or no distortion, yet are separated by only one clad thickness. This is a significant fact since in these fibers the core glass melts at a lower temperature than the clad.

CONCLUSION

As a result of the three-month effort we have found that (1) Good welds require stress-free fibers or fibers which are completely restrained; (2) Good welds also require sufficient power

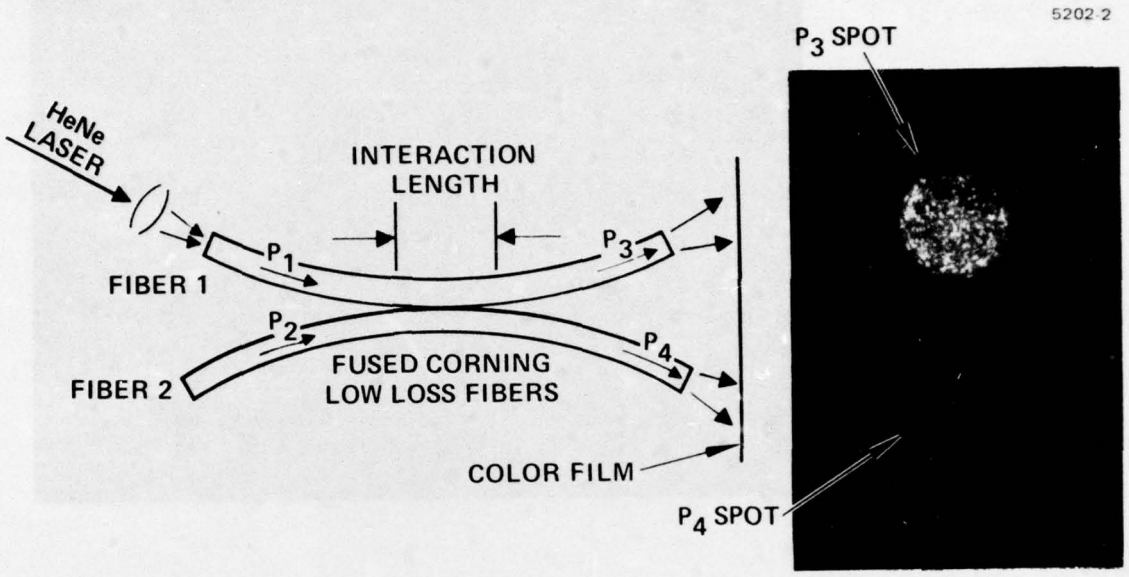

Fig. 4. Schematic illustration of two fused fibers with a He-Ne laser exciting the main channel fiber. Photograph of the output.

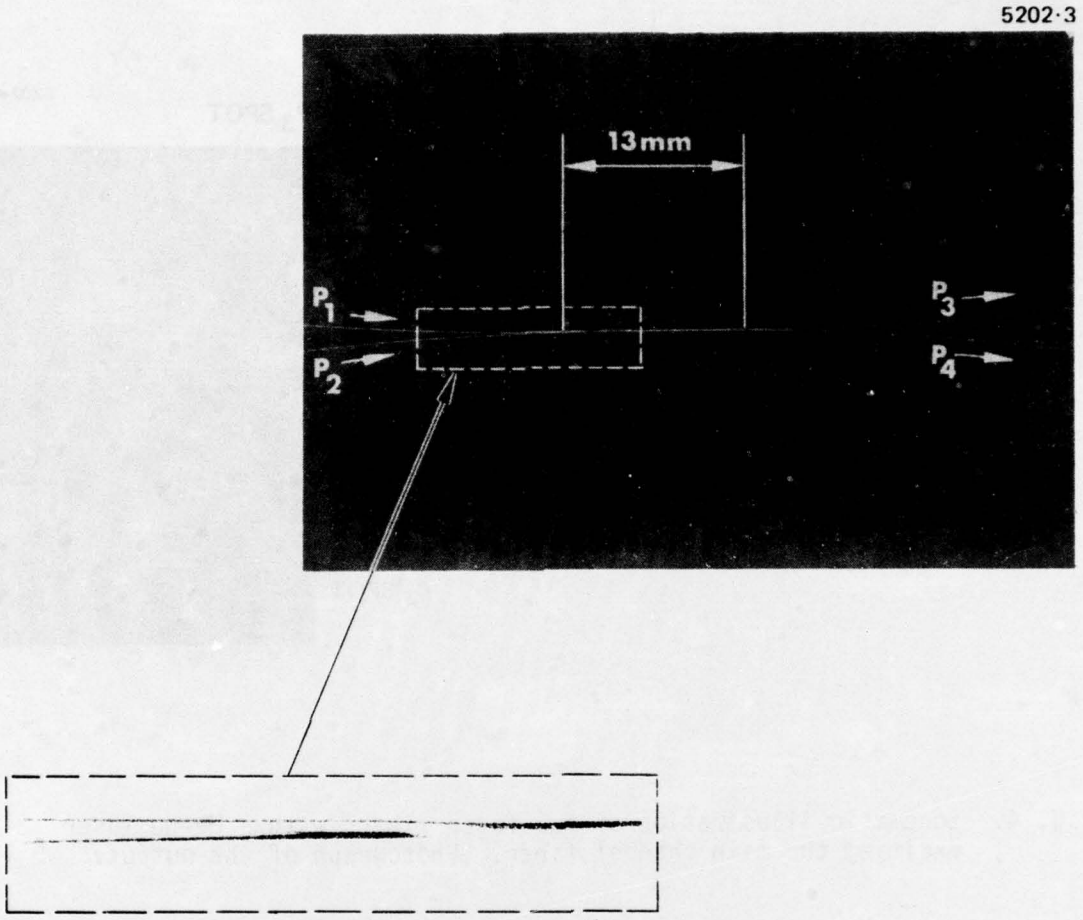

Fig. 5. Photograph of coupler number 32. Magnified photo of the region where the two fibers join.

4975-1

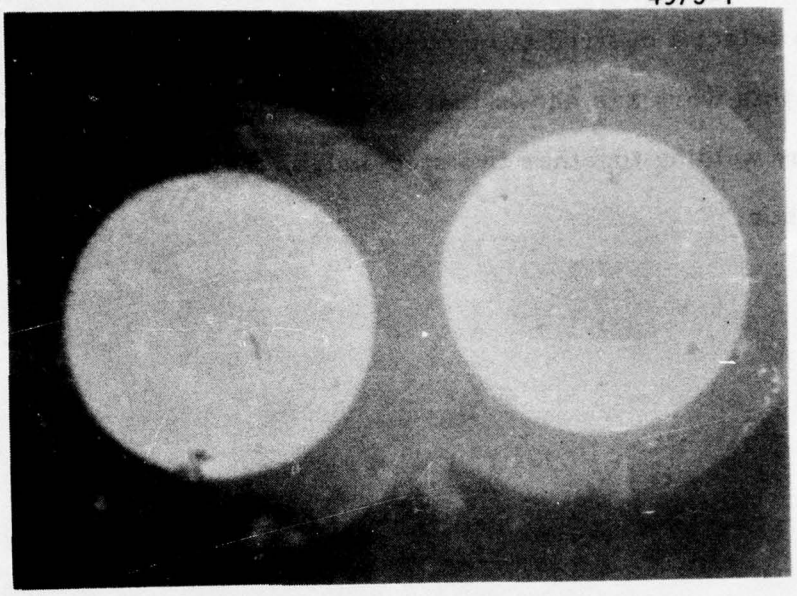

Fig. 6. Photomicrograph at a cleaved cross section of two welded fibers.

density for quick welds and a cylindrical lens for a correctly shaped beam; (3) Further effort is needed to reduce insertion loss and to be able to select a desired tap percentage; and finally (4) most important is that this work has shown that an efficient access coupler can be made by welding together two step-index, multimode fibers using a CO_2 laser.

☆ U. S. GOVERNMENT PRINTING OFFICE: 1976 — 757-001/19